Biochemical Pharmacology 183 (2021) 114317

Contents lists available at ScienceDirect

Biochemical Pharmacology

journal homepage: www.elsevier.com/locate/biochempharm

Targeting of HER/ErbB family proteins using broad spectrum Sec61 inhibitors coibamide A and apratoxin A

Soheila Kazemi [a,e], Shinsaku Kawaguchi [b], Christian E. Badr [c], Daphne R. Mattos [a], Ana Ruiz-Saenz [d,1], Jeffrey D. Serrill [a], Mark M. Moasser [d], Brian P. Dolan [e], Ville O. Paavilainen [f], Shinya Oishi [b,2], Kerry L. McPhail [a], Jane E. Ishmael [a,*]

[a] Department of Pharmaceutical Sciences, College of Pharmacy, Oregon State University, Corvallis, OR 97331, USA
[b] Graduate School of Pharmaceutical Sciences, Kyoto University, Sakyo-ku, Kyoto 606-8501, Japan
[c] Department of Neurology, Neuro-Oncology, Division, Massachusetts General Hospital, Harvard Medical School, 149 13th Street, Charlestown, MA 02129, USA
[d] Department of Medicine, Helen Diller Family Comprehensive Cancer Center, University of California, San Francisco, CA, USA
[e] Department of Biomedical Sciences, Carlson College of Veterinary Medicine, Oregon State University, Corvallis, OR 97331, USA
[f] Institute of Biotechnology, University of Helsinki, Helsinki 00014, Finland

ARTICLE INFO

Keywords:
ErbB
HER
Signal peptide
Kinase inhibitor
Coibamide A
Apratoxin A

ABSTRACT

Coibamide A is a potent cancer cell toxin and one of a select group of natural products that inhibit protein entry into the secretory pathway via a direct inhibition of the Sec61 protein translocon. Many Sec61 client proteins are clinically relevant drug targets once trafficked to their final destination in or outside the cell, however the use of Sec61 inhibitors to block early biosynthesis of specific proteins is at a pre-clinical stage. In the present study we evaluated the action of coibamide A against human epidermal growth factor receptor (HER, ErbB) proteins in representative breast and lung cancer cell types. HERs were selected for this study as they represent a family of Sec61 clients that is frequently dysregulated in human cancers, including coibamide-sensitive cell types. Although coibamide A inhibits biogenesis of a broad range of Sec61 substrate proteins in a presumed substrate-nonselective manner, endogenous HER3 (ErbB-3) and EGFR (ErbB-1) proteins were more sensitive to coibamide A, and the related Sec61 inhibitor apratoxin A, than HER2 (ErbB-2). Despite this rank order of sensitivity (HER3 > EGFR > HER2), Sec61-dependent inhibition by coibamide A was sufficient to decrease cell surface expression of HER2. We report that coibamide A- or apratoxin A-mediated block of HER3 entry into the secretory pathway is unlikely to be mediated by the HER3 signal peptide alone. HER3 (G11L/S15L), that is fully resistant to the highly substrate-selective cotransin analogue CT8, was more resistant than wild-type HER3 but only at low coibamide A (3 nM) concentrations; HER3 (G11L/S15L) expression was inhibited by higher concentrations of either natural product. Time- and concentration-dependent decreases in HER protein expression induced a commensurate reduction in AKT/MAPK signaling in breast and lung cancer cell types and loss in cell viability. Coibamide A potentiated the cytotoxic efficacy of small molecule kinase inhibitors lapatinib and erlotinib in breast and lung cancer cell types, respectively. These data indicate that natural product modulators of Sec61 function have value as chemical probes to interrogate HER/ErbB signaling in treatment-resistant human cancers.

1. Introduction

Genes encoding membrane-bound and secreted proteins represent approximately one third of the protein-coding genome, and are enriched in what has been described as the druggable proteome [1]. Extensive mapping of proteins targeted by FDA-approved small molecule and technology-based medicines, as of 2015, predicted 70% of known drug targets to be either secreted, multi-pass or single-pass membrane proteins [1]. Most membrane-bound and secreted proteins are processed and sorted through the conventional ER-to-Golgi secretory pathway [2]. Typically, an N-terminal cleavable signal sequence or a transmembrane segment within a nascent polypeptide is detected by the cytosolic signal

* Corresponding author.
E-mail address: jane.ishmael@oregonstate.edu (J.E. Ishmael).
[1] Department of Cell Biology, Erasmus University Medical Center, Rotterdam, The Netherlands.
[2] Kyoto Pharmaceutical University, Kyoto, Japan

https://doi.org/10.1016/j.bcp.2020.114317
Received 2 August 2020; Received in revised form 29 October 2020; Accepted 30 October 2020
Available online 3 November 2020

recognition particle (SRP), which then targets the ribosome-nascent chain (RNC) complex to the surface of the rough ER through association with the SRP receptor at the ER membrane [3]. The RNC is subsequently transferred, in a GTP-dependent manner, to the Sec61 translocation channel and upon recognition of the signal peptide the Sec61 channel opens, allowing translocation of the polypeptide across the ER membrane. Using this mechanism, nascent polypeptides may pass directly into the ER lumen or, in the case of integral membrane proteins, move laterally into the ER membrane via the Sec61 translocon lateral gate, which essentially marks the entrance to the secretory compartment of the cell [3–5]. Numerous signaling events subsequently ensure correct folding, post-translational modification and forward trafficking of diverse arrays of mature proteins to different final destinations such as the cell exterior (for secreted growth factors or cytokines), the plasma membrane (for cell surface receptors) or ER or Golgi compartments (for ER resident- or Golgi-located proteins).

Receptor tyrosine kinases (RTKs) are a superfamily of integral membrane proteins that are directed to the secretory pathway early in their biosynthesis. An understanding of this process is important as the availability of functional RTK receptors at the cell surface is ultimately regulated by the rate of new protein synthesis relative to the rate of receptor internalization at the plasma membrane [6]. Although these receptors are critical for normal cell function, their dimerization partners, the endogenous ligands that activate them, and signal transduction pathways have been the focus of intense research to advance the treatment of human cancer [7]. The human epidermal growth factor receptor (HER) family of RTKs, and associated downstream signaling pathways, was one of the first RTK sub-families to be targeted by mechanism-based cancer therapies [8,9]. For example, amplification or mutational activation of HER family receptors discovered in lung [10,11], brain [12–14], and breast [15–18] cancers, and advances in the understanding of the HER signaling network, has led to the development of numerous HER-targeted therapies approved for use in a range of cancers with aberrant HER signaling [9]. Of the four receptors that comprise the HER family, epidermal growth factor receptor (EGFR; ErbB-1), HER2 (ErbB-2), HER3 (ErbB-3) and HER4 (ErbB-4), most FDA-approved drugs directly target the function of EGFR or HER2 [9,19]. These therapeutics include monoclonal antibodies, designed to block ligand-induced activation or dimerization of HER receptors by targeting their extracellular domains, and small molecule kinase inhibitors that penetrate the cell to inhibit receptor catalytic function. Although originally conceived as effective single agent medicines, in practice multiple compensatory mechanisms drive acquired resistance to HER-targeted drugs in a pattern similar to that seen with cytotoxic chemotherapeutic agents [20]. In addition, both acquired and intrinsic drug resistance highlights a continued need for development of new cancer therapies to improve, or for use in combination with, standard of care [20,21].

In 2015 the Moasser laboratory described a fundamentally different way to eliminate the function of the HER3 protein [22]. Using a small molecule inhibitor of the Sec61 protein translocation channel, termed CT8, they demonstrated that HER3 expression could be selectively suppressed post-transcriptionally in human HER2-amplified breast cancer cells while sparing expression of the other three members of the HER family [22]. CT8 binds to the Sec61 protein translocon in a manner that prevents signal peptide recognition and opening of the Sec61 channel [23]. Binding of CT8 inhibits cotranslational translocation of only a relatively select set of Sec61 substrate proteins, including HER3, and thereby blocks the ability of the nascent proteins to enter the secretory pathway [23]. Consistent with the action of other Sec61 inhibitors [24,25], CT8 was found to induce proteasomal degradation of HER3 in breast cancer cells as a consequence of Sec61 inhibition [22]. This demonstration of targeted elimination of HER3 by a selective Sec61 inhibitor, was significant as HER3 is an essential oncogenic driver in HER2-amplified human cancers but has historically been difficult to target [19,26–28]. The kinase domain of HER3 is catalytically inactive, yet this receptor is a strong activator of PI3K/Akt signaling and forms a HER2-HER3 complex that is resistant to inhibition by classic HER2-targeted kinase inhibitors [29–34]. Although co-translational translocation of HER2, and therefore HER2 expression, is not disrupted by CT8, the CT8-induced loss of HER3 was shown to dramatically suppress HER2-HER3 signaling in HER2-amplified BT474 breast cancer cells [22]. Further, CT8 alone was minimally toxic to BT474 cells, but when combined with a HER2-directed kinase inhibitor, lapatinib, this combination induced a significant increase in apoptotic cells [22]. This ability of CT8 to increase the cytotoxic efficacy of a validated HER2 inhibitor highlighted the future potential for pharmacological manipulation of the HER family in human cancer cells through direct modulation of Sec61 activity.

CT8 is a member of a class of synthetic cyclic depsipeptides known as cotransins that were developed through rational design as simplified analogues of the fungal natural product HUN-7293 [24,35]. HUN-7293 is a complex heptadepsipeptide that was discovered as an inhibitor of vascular cell-associated adhesion molecule expression [36,37], and subsequently found to be a specific inhibitor of the Sec61 translocon channel [25]. The cotransins impact secretory pathway protein biogenesis due to their ability to block signal-peptide recognition of Sec61 substrates in a manner that can be relatively substrate-selective, or broad-ranging, depending on the specific cotransin molecular structure [38,39,22–25]. Although molecules based on the HUN-7293 scaffold have been the most extensively studied using chemical biology approaches, several other naturally-occurring molecules have since been found to directly target Sec61-mediated protein translocation [40]. These compounds include: decatransin [41] from the fungus *Chaetospharia tulasneorum*, virulence factor mycolactone produced by *Mycobacterium ulcerans* [42,43],ipomoeassin F from the plant *Ipomoea squamosa* [44], and apratoxin A from the marine cyanobacterium *Moorea producens* [45–48]. In previous studies, we determined that the potent anticancer compound coibamide A, also from a marine cyanobacterium, is functionally similar to apratoxin A [49–51] and binds Sec61 at a site that is partially shared with other Sec61 inhibitors [40,52]. Coibamide A was discovered in a screen for new chemical entities with anticancer activity and displayed potent activity against many human cancer cell lines including those representing triple-negative breast cancers [49]. In follow up studies, coibamide A showed evidence of dual targeting of a RTK ligand-receptor pair and anti-angiogenic potential within hours of exposure [50]. Coibamide A inhibited secreted levels of vascular endothelial growth factor A (VEGFA) and decreased steady state expression of vascular endothelial growth factor receptor 2 (VEGFR2) with low nanomolar potency [50]. Given the sensitivity of breast cancer cell types to coibamide A, the main goal of the present study was to determine if, and to what extent, expression of the HER family of RTKs is modulated by coibamide A. We also compared the action of coibamide A and apratoxin A (Fig. 1) as these complex cytotoxic natural products have non-identical binding sites [52], and thus the two could be anticipated, *a priori*, to have different selectivity profiles for Sec61 substrates in cells.

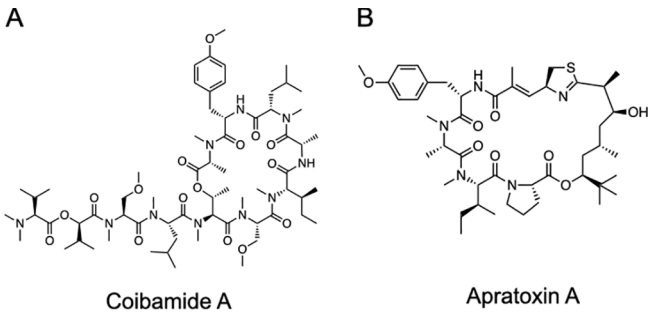

Fig. 1. Chemical structures of the marine natural products: (A) coibamide A and (B) apratoxin A.

2. Materials and methods

2.1. Chemicals, reagents, and antibodies

Natural product coibamide A was isolated and purified as described previously [49], following re-collection of biological material by hand using SCUBA from Coiba National Park, Panama. Synthetic coibamide A was prepared at Kyoto University (Japan) according to the procedure described previously [52]. The materials for solid-phase peptide synthesis were provided from Watanabe Chemical Industries (Hiroshima, Japan) and FUJIFILM Wako Pure Chemical Corporation (Osaka, Japan). The product was characterized by 1D and 2D NMR comparison with the natural product (Bruker AVANCE III 700 spectrometer with cryoprobe) and as follows: $[\alpha]_{23}^{D}$ –60 (*c* 0.1, $CHCl_3$); HRMS (ESI-TOF) calculated for $C_{65}H_{110}N_{10}O_{16}Na$ $[M + Na]^+$: 1309.7993; found: 1309.7994. The isolation and purification of apratoxin A from a Red Sea strain of *Moorea producens* has been described previously [53]. Coibamide A and apratoxin A were reconstituted in 100% cell culture-grade DMSO Millipore-Sigma (Burlington, MA), aliquoted and stored in amber borosilicate glass vials at −20 °C for use in biological studies. Bortezomib was purchased from Cell Signaling Technology, Inc. (Danvers, MA), coelenterazine was from Promega Corporation (Madison, WI), erlotinib was from Enzo Life Sciences (Farmingdale, NY) and rapamycin A, brefeldin A and lapatinib were from Millipore-Sigma. All compounds from commercial sources were also reconstituted in 100% DMSO and stored at −20 °C. Final concentrations of DMSO for *in vitro* studies never exceeded 0.1%. For studies in 96- or 384-well plates, compounds were delivered using an Hewlett-Packard (HP) D300 Digital Dispenser with HP Dispensing Software (version 3.2.2). General laboratory reagents for biological studies and natural product extraction and purification were from VWR International (Radnor, PA). HPLC-grade solvents were used for all natural product isolations. All antibodies were from commercial sources and were used according to the recommended protocols.

2.2. Mammalian cell culture

Human MDA-MB-231, MDA-MB-468, MDA-MB-436, HS-578T, BT-474, MCF-7 breast cancer cells, 11–18, PC-9 lung cancer cell lines cells, and HEK-293T human embryonic kidney cells were from the American Type Culture Collection (ATCC, Manassas, VA). Human 293FT cells, for generation of lentivirus, were from Thermo Fisher Scientific (Waltham, MA). Human 11–18 and PC-9 lung cancer cells were a kind gift from Dr. Monika Davare (Oregon Health & Science University, Portland. OR). Upon receipt all mammalian cell lines were expanded and banked in cryogenic storage at low passage number to restrict the number of passages (≤15), and therefore time in culture, of working stocks relative to the validated reference stocks. 293FT cells were cultured in Dulbecco's Modified Eagle's Medium (DMEM) with 10% fetal bovine serum (FBS; Hyclone, Logan, UT), 0.1 mM MEM non-essential amino acid solution, L-glutamine (6 mM), sodium pyruvate (1 mM), 100 U/mL penicillin, and 100 mg/mL streptomycin (1% penicillin/streptomycin), and Geneticin™ selective antibiotic. All triple-negative breast cancer cells were cultured in Minimum Essential Medium (MEM) with Earl's salts and L-glutamine (Corning Life Sciences), supplemented with 10% FBS and 1% penicillin/streptomycin. BT-474 cells were cultured in Hybri-Care medium with L-Glutamine and HEPES, supplemented with 1% penicillin/streptomycin and 10% FBS. MCF-7 cells were cultured in RPMI 1640 medium with GlutaMAX™ (20 mM) and 7.5. % FBS. HEK-293T cells were cultured in DMEM supplemented with 10% FBS, L-glutamine (2 mM) and 1% penicillin/streptomycin and 11–18 and PC-9 lung cancer cells were cultured in RPMI 1640 medium with 10% FBS and 1% penicillin/streptomycin. All cells were grown under standard conditions and maintained at 37 °C in an atmosphere of 5% CO_2.

2.3. Plasmids, lentiviral expression, transduction and transfection

Gaussia luciferase (Gluc) was cloned in CSCW, a self-inactivating lentivirus vector, under the control of the cytomegalovirus (CMV) immediate early promoter as previously described (Sena-Esteves 2004); this promoter also controls the expression of CFP separated from Gluc by an internal ribosome entry site (IRES). Lentiviral vectors were constructed by co-transfecting 293-FT cells with this plasmid and ViraPower™ Lentiviral Packaging Mix using Lipofectamine™ 2000 (Thermo Fisher Scientific). The supernatant containing the lentivirus was harvested after 72 h, concentrated (Amicon® centrifugal filters) and the titer quantified as transducing units/mL. MDA-MB-231 cells were then infected with lentivirus in the presence of 8 μg/mL Polybrene® (Sigma-Aldrich) and transduction efficiency confirmed by counting CFP-positive cells 48 h post-infection. The construction of cDNA constructs in pCDNA-DEST40 vectors (Thermo Fisher Scientific) for expressing C-terminally expressed V5-tagged proteins in mammalian cells has been described previously [22]. EGFR, HER2, HER3, HER4 and a HER3 signal peptide mutant (HER3 G11L/S15L) were transiently expressed in HEK293T cells using jetPRIME™ transfection reagent (Polyplus transfection, New York) according to manufacturer's protocol.

2.4. Gaussia luciferase (Gluc) secretory assay

For concentration–response assays, 3,000 stably Gluc-expressing MDA-MB-231 cells per well were seeded in 96-well plates and allowed to grow overnight. The next day, seeding medium was replaced with complete medium containing test compounds or vehicle and plates returned to the incubator. Following a 16 h treatment, 20 μL of conditioned cell culture medium was removed from each well and transferred to 96-well white-walled plates. Subsequently, 50 μL of 1.68 μM coelenterazine was injected into each well for a final concentration of 1.2 μM, and luminescent signals were measured using a multi-mode microplate reader (BioTek Synergy HT) with Gen5® software and compared across conditions (3 sec wait, 0.5 sec integration time following coelenterazine injection).

2.5. Cell viability and caspase activation assays

For viability assays, cells were seeded in 384-well, white-walled tissue culture plates at a density of 800 cells/well or 96-well culture plates at a density of 3,000 cells/well. After 18 h, cells were treated with coibamide A (0.3 nM−300 nM) or vehicle (0.1% DMSO). For drug combination studies, cells were co-treated with, or without, coibamide A plus lapatinib or erlotinib (0.03 nM–300 nM). Cell viability was assessed at the end of treatment using a CellTiter-Glo® luminescent cell viability assay (# G7572; Promega Corp., Madison, WI) using a multi-mode microplate reader (as above). The viability of vehicle-treated cells was defined as 100% in all studies. For analysis of caspase activity, cells were seeded into clear bottom white-walled plates (Greiner CellStar®) and caspase 3/7 activation assessed using a Caspase-Glo® 3/7 luminescent assay (Promega Corp.).

2.6. Western blot analysis

After treatment culture plates were placed on ice and cells rinsed with phosphate-buffered saline (PBS), lysed and processed as described previously [54]. Cell lysates were adjusted for protein content using a bicinchoninic assay (BCA), mixed with Laemmli sample buffer so that equal amounts of protein could be separated by SDS-PAGE and immobilized onto PVDF membranes. Membranes were subsequently blocked in 5% (w/v) non-fat dry milk in 50 mM Tris-HCl, pH 7.4, 150 mM NaCl (TBS) plus 0.1% Tween-20 (TBS-Tween), and then incubated for overnight at 4 °C with the appropriate primary antibody. The following day, membranes were washed in TBS-Tween (3 × 10 min) and incubated with an HRP-conjugated secondary antibody (goat anti-rabbit IgG

#7074 Cell Signaling Technology Inc.) for 1 h at room temperature. Finally, membranes were washed again in TBS-Tween (4 × 5 min), and proteins revealed using a chemiluminescence reaction (Amersham ECL reagent, GE Healthcare, Chicago, IL). Images were captured using a MyECL image analysis system (Thermo Fisher Scientific). Codes for primary antibodies from Cell Signaling Technology, Inc. were as follows: EGF Receptor (D38B1) XP® rabbit mAb (#4267 detects a specifc band corresponding to the mature form of the receptor at 175 kDa), HER2/ErbB2 (D8F12) XP® rabbit mAb (#4290 detects a specifc band corresponding to the mature form of the receptor at 185 kDa), HER3/ErbB3 (D22C5) XP® rabbit mAb (#12708 detects a specifc band corresponding to the mature form of the receptor at 185 kDa), V5-Tag (D3H8Q) rabbit mAb (#13202 detects only transfected proteins tagged with a V5 epitope), GAPDH (D16H11) XP® rabbit mAb (#5174 detects a specifc band at 37 kDa), α-Tubulin (11H10) rabbit mAb (#2125 detects a specifc band at 52 kDa), PARP (46D11) rabbit mAb (#9532 detects specifc bands at 116 and 89 kDa), Caspase-3 (8G10) rabbit mAb (#9665 detects both full-length caspase at 35 kDa and the large fragment 17/19 kDa corresponding to cleaved caspase 3), β-Actin (13E5) rabbit mAb (#4970 detects a specifc band at 45 kDa), Phospho-Akt (Thr308) rabbit polyclonal antibody (#9275 detects only the Thr308 phosphorylated form of Akt at 60 kDa), Phospho-Akt (Ser473) polyclonal antibody (#9271 detects only the Ser473 phosphorylated form of Akt at 60 kDa), Akt (pan) (C67E7) rabbit mAb (#4691 detects a specific band at 60 kDa), S6 Ribosomal Protein (5G10) rabbit mAb (#2217 detects a specific band at 32 kDa), Phospho-S6 Ribosomal Protein (Ser235/236) rabbit polyclonal antibody (#2211 detects only the Ser235/236 phosphorylated form at 32 kDa), p44/42 MAPK (Erk1/2) (137F5) rabbit mAb (#4695 detects specific bands at 42 and 44 kDa) and Phospho-p44/42 MAPK (Erk1/2) (Thr202/Tyr204) (20G11) rabbit mAb (#4376 detects only the dually Thr202/Tyr204 phosphorylated forms of MAPK at 42 and 44 kDa, or single phosphorylated form at Thr202).

2.7. Flow cytometric analysis of surface HER2

MCF-7 breast cancer cells were seeded in 6-well tissue culture plates at a density of 5×10^5 cells/well and allowed to grow overnight. The next day, cells were treated with coibamide A (10 nM−100 nM), brefeldin A (5 μM) or vehicle (0.1% DMSO) for 18 h, harvested with trypsin and rinsed in cold Hank's Balanced Salt Solution (HBSS; Thermo Fisher Scientific) supplemented with 0.1% BSA (Amresco, Albany, NY). For cell surface detection of HER2, cells were stained with PE anti-human erbB2/HER-2 mouse mAb (# 324406; BioLegend, San Diego, CA) or PE mouse IgG1, k isotype control (FC) mouse mAb (# 400113; BioLegend) for 30 min at 4 °C, washed once and resuspended in HBSS/0.1% BSA solution. All cell samples were analyzed by flow cytometry using an Accuri C6 flow cytometer (BD Biosciences, San Jose, CA) and flow cytometry data analyzed with FlowJo Software (FlowJo LLC, BD Biosciences).

2.8. Data analysis

Concentration-response relationships were analyzed using Graphpad Prism Software version 8.0 (GraphPad Software Inc., San Diego, CA), and EC_{50} values derived using nonlinear regression analysis fit to a logistic equation. Statistical significance of cell viability was assessed using a one-way analysis of variance (ANOVA) followed by a student's *t*-test to compare control and treatment groups. P-values of < 0.05 were considered as statistically significant. Protein expression was quantified by densitometry. The intensity of each band was normalized to the loading control and quantified relative to controls using Image J software (http://rsbweb.nih.gov/). Analysis of potential synergy between coibamide A and kinase inhibitors was determined using the Chou-Talay Combination Index method with CompuSyn (CompuSyn Inc., Paramus, NJ) software [55]. Fraction affected (Fa) values were calculated from mean cell viability of technical replicates (subtracted from 1 for each condition). As the experimental design resulted in non-constant ratios for combination mixtures data were expressed as normalized isobolograms [56].

3. Results

3.1. Coibamide A inhibits protein secretion, EGFR expression and viability of triple-negative breast cancer cells

The pharmacological specificity of coibamide A as an inhibitor of secretory function was first tested in a whole cell assay based on bioluminescence detection of a secreted reporter *Gaussia luciferase* (Gluc) reporter in the presence of the natural product. For these studies, MDA-MB-231 breast cancer cells were infected with a lentiviral construct encoding Gluc that, upon transduction, is expressed, trafficked and secreted into medium of living cells [57]. In this assay, exposure of an aliquot of Gluc-conditioned medium to the substrate coelenterazine results in a bioluminescent reaction which was quantified to determine the extent of Gluc expression relative to vehicle-treated control cells [57]. The secretory function of Gluc-expressing MDA-MB-231 (Gluc-MDA-MB-231) cells was assessed in the presence of varying concentrations of coibamide A (0.1 nM−300 nM), apratoxin A (0.1 nM–300 nM), rapamycin A (1 nM−3 μM) or vehicle (0.1% DMSO). After 16 h, coibamide A potently inhibited the secretory function of Gluc-MDA-MB-231 cells in a pattern comparable to apratoxin A (Fig. 2A). The IC_{50} values for inhibition of Gluc were 7.6 ± 0.2 nM and 1.0 ± 0.1 nM for coibamide A and apratoxin A, respectively. In contrast, rapamycin produced no specific change in the secretory function of Gluc-MDA-MB-231 cells consistent with the known mechanism of rapamycin action outside the secretory pathway (Fig. 2A). These observed changes in secretory function occurred within a time frame that coibamide A is relatively non-toxic to both primary and cancer cells [49,50]. Consistent with previous studies, coibamide-induced cytotoxicity to HEK293T cells was also time-dependent and thus treatment times of up to 24 h were selected to study expression of endogenous and over-expressed HER proteins in response to Sec61 inhibition (Fig. 2B). As triple-negative breast cancers lack HER2 but can be EGFR positive [58], we studied the effect of coibamide A on EGFR protein expression. Immunoblot analysis of MDA-MB-231 or MDA-MB-468 cell lysates treated with or without the natural product revealed a concentration-dependent decrease in EGFR expression by 24 h (Fig. 2C to F) and declined steadily as a function of treatment time (Fig. 3D).

Although early studies indicated that triple-negative MDA-MB-231 cells undergo apoptosis in response to coibamide A [49,50], the relatively limited supply of the field-collected natural product had prevented further biological evaluation. With refinement of routes for total synthesis and a revision of the stereochemistry [59–61], we were able to evaluate the cytotoxic potential of synthetic coibamide A against an expanded panel of triple-negative breast cancer cells with varying basal EGFR expression. Coibamide A was synthesized in the laboratory of Professor Shinya Oishi (Kyoto Pharmaceutical University) and verified as identical to the natural product based on high resolution mass data, specific optical rotation, overlay of ^{1}H and ^{13}C NMR data with the natural product data, and Marfey's analysis of key residues [52]. Next, we treated, MDA-MB-468, MDA-MB-231, MDA-MB-436, HS-578T, and a representative HER2-amplified breast cancer cell type (BT-474) with increasing concentrations of coibamide A or vehicle (0.1% DMSO) for 72 h and evaluated effects on cell viability by quantification of cellular ATP as a readout of metabolic status. Synthetic coibamide A induced a concentration-dependent decrease in the viability of all five breast cancer cell types, relative to vehicle-treated cells with EC_{50} values ranging from 0.4 nM to 4 nM (Table 1). Coibamide A was not selective against triple-negative breast cancer cells, however MDA-MB-468 cells with high expression of EGFR were one of the most sensitive (Fig. 3A and B) and therefore selected for further evaluation. MDA-MB-468 cells were exposed to synthetic coibamide A (3 nM and 10 nM) or vehicle (0.1%

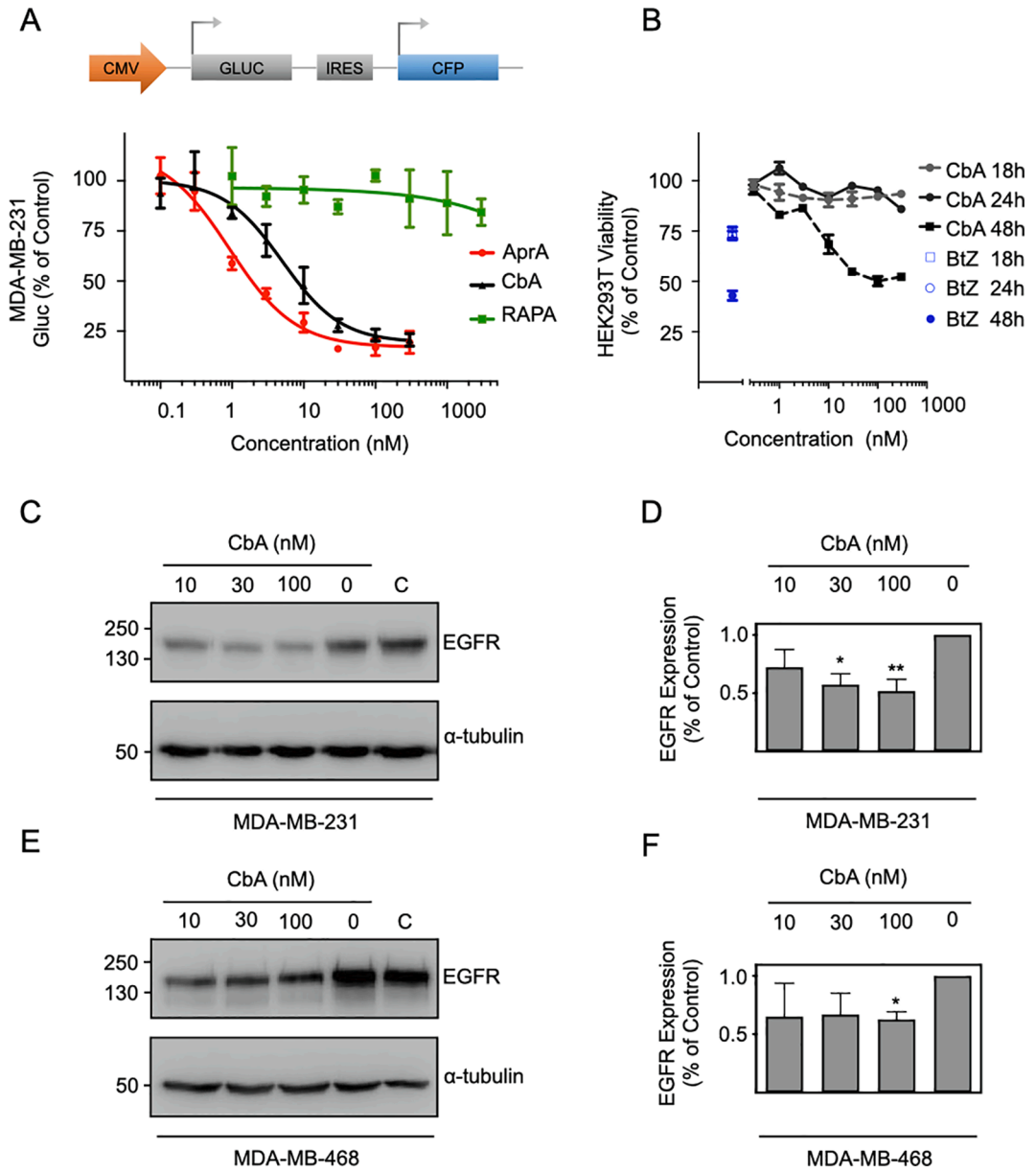

Fig. 2. Coibamide A and Apratoxin A inhibit the secretory function of MDA-MB-231 breast cancer cells. (A) Effect of coibamide A on cellular secretory function. Human MDA-MB-231 breast cancer cells were infected with a lentiviral vector encoding *Gaussia luciferase* (Gluc) under the control of a CMV promoter. MDA-MB-231 cells expressing Gluc were treated with, or without (0.1% DMSO), coibamide A (CbA), apratoxin A (AprA) or rapamycin A (RAPA) and Gluc activity was assayed from aliquots of the conditioned medium after 16 h. Data points show mean luminescence values ± SE (n = 3 wells per treatment) expressed as percentage (%), relative to vehicle-treated cells, from a comparison repeated at least three times independent experiments. (B) Time-dependent changes in the viability of representative non-breast cancer cells in response to coibamide A. HEK293T cells were exposed to increasing concentrations of coibamide A (CbA), bortezomib (BtZ; 300 nM) or vehicle (0.1% DMSO) for 18, 24 or 48 h. Data points show mean viability ± SE (n = 3 wells per treatment), relative to vehicle-treated cells, from a comparison that was repeated three times. (C) Immunoblot analysis of EGFR receptor and α-tubulin expression in MDA-MB-231 and (E) MDA-MB-468 cells treated with, or without (untreated = C), coibamide A (10, 30 or 100 nM) or 0.1% DMSO (0) for 24 h. Images are representative of the loading control (α-tubulin) relative to EGFR expression. (D and F) Quantification of immunoblot data shown in C and E from three independent experiments. Bars represent intensity of bands ± SE normalized to α-tubulin, relative to vehicle-treated cells (0). Statistical significance is indicated as: * $P < 0.01$, ** $P < 0.001$.

DMSO) for up to 72 h and evaluated for evidence of caspase-3,7 activation and markers of apoptosis. Coibamide A treatment resulted in a statistically significant and concentration-dependent increase in caspase-3,7 activity at 48 h, 60 h and 72 h relative to vehicle-treated cultures (Fig. 3C). In separate studies, adherent (A) and any floating or detaching (D) cells were collected up to 72 h after treatment with, or without, coibamide A (10 nM) and probed for expression of EGFR and apoptotic cell death biomarkers: poly(ADP-ribose) polymerase 1 (PARP1) and caspase 3 (Fig. 3D). Consistent with decrease in EGFR observed on exposure to the field-collected natural product (Fig. 2C and D), synthetic coibamide A induced a statistically significant time-dependent decrease in EGFR expression in adherent cells over 72 h (Fig. 3D and E). The adherent MDA-MB-468 cell population showed no significant changes in expression of full-length PARP1 and caspase-3 over this time frame and lacked immunoreactivity corresponding to cleaved PARP1 and cleaved caspase 3 that was observed only in detached cells (Fig. 3D and E).

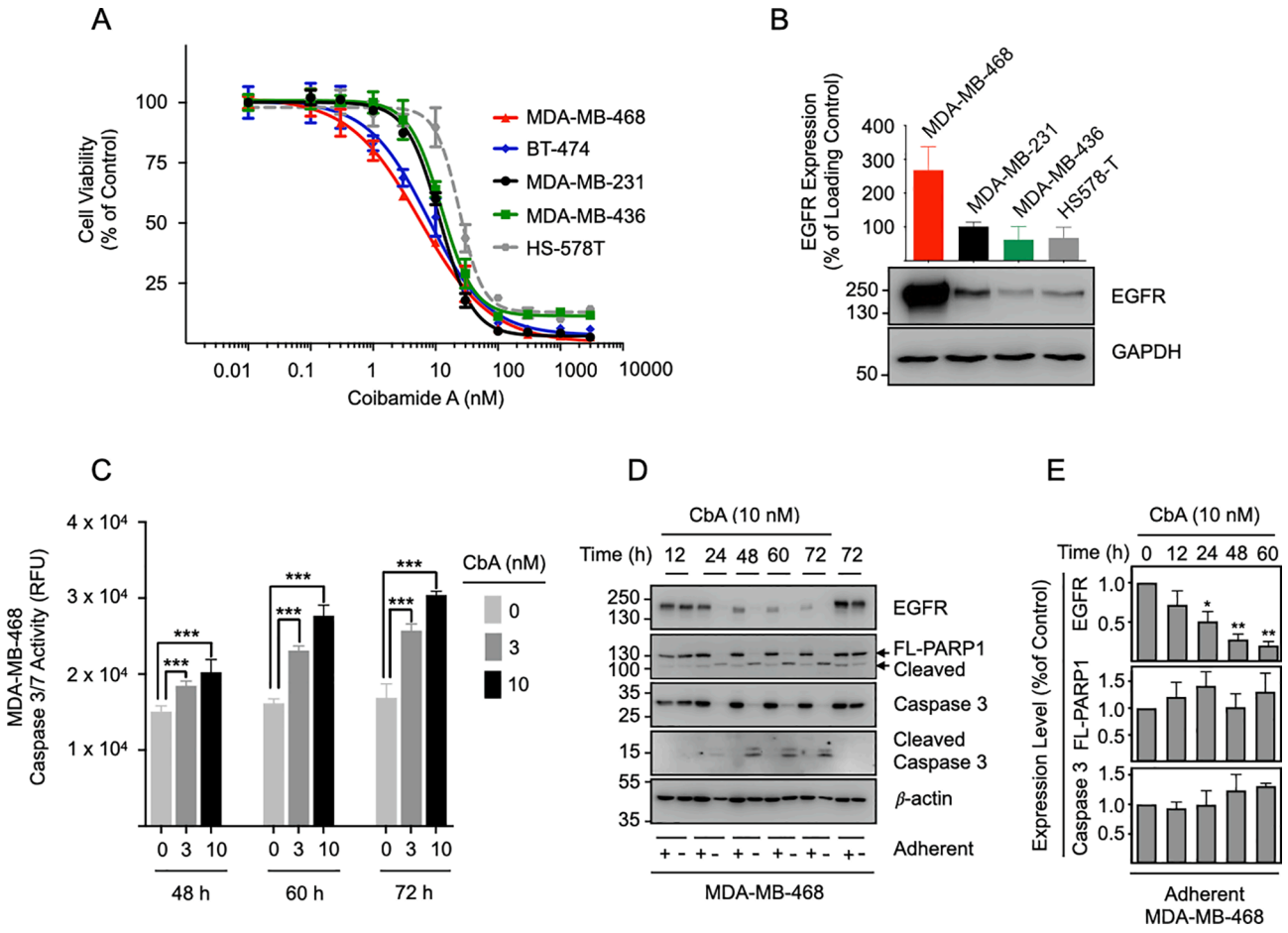

Fig. 3. Coibamide A is cytotoxic to triple-negative and HER2 positive breast cancer cell types. (A) Concentration-response relationship for coibamide-induced reduction of viability in triple-negative (MDA-MB-468, MDA-MB-231, MDA-MB-436, HS-578T) and HER2-amplified (BT-474) breast cancer cells. Cells were exposed at the same time to increasing concentrations of coibamide A, or vehicle (0.1% DMSO), for 72 h and cell viability determined using a Cell-Titer Glo® luminescent assay. Graph shows a single comparison of cell types that was repeated three times. (B) Immunoblot shows basal EGFR expression in untreated triple negative breast cancer cell types used in panel A. Bars represent quantification of EGFR intensity relative to GAPDH. (C) Time and concentration-dependent analysis of caspase-3,7 activity in MDA-MB-468 cells treated with, or without (0.1% DMSO), 3 nM or 10 nM coibamide A for 48, 60 and 72 h. Bars represent mean relative fluorescence units (RFU) ± SE from three independent determinations. (D) Immunoblot analysis of EGFR, PARP1 and caspase-3 expression relative to β-actin in floating and adherent cells exposed to coibamide A, or vehicle (0.1% DMSO), for 12 h to 72 h as indicated. Blots are representative of an experiment repeated at least three times with the same result. (E) Quantification of immunoblot data for EGFR, full length PARP1 and caspase-3 intensity relative to control in the adherent cell population shown in panel D from three independent experiments. Statistical significance is indicated as: * $P < 0.01$, ** $P < 0.001$ *** $P < 0.0001$.

Table 1
Cytotoxicity of Coibamide A to human breast cancer cells.

Breast cancer cell type	Characteristics	EC_{50} ± S.E. (nM)
MDA-MB-231	Triple-Negative	1.0 ± 0.2
MDA-MB-436	Triple-Negative	0.9 ± 0.3
MDA-MB-468	Triple-Negative	0.4 ± 0.1
HS578T	Triple-Negative	4.0 ± 0.9
BT474	HER2 positive	0.8 ± 0.2

Cell viability was assessed after 72 h relative to vehicle-treated cells. Concentration-response data were analyzed using GraphPad Prism Software version 6.0 (GraphPad Software Inc., San Diego, CA), and EC_{50} values derived using nonlinear regression analysis fit to a logistic equation. Results represent mean ± S.E. from three independent experiments.

3.2. Endogenous HER family members are differentially sensitive to coibamide A

As CT8 preferentially targets biosynthesis of HER3 among HER family members [22], we next tested the ability of coibamide A to inhibit expression of HER2 and HER3 in a representative HER2-amplified cell type. BT-474 cells were treated with increasing concentrations of coibamide A (10 to 100 nM) or vehicle (0.1% DMSO), for 24 h and cell lysates harvested for analysis of endogenous HER protein expression. This analysis revealed a pattern of differential HER sensitivity in response to treatment. Coibamide A induced statistically significant decreases in EGFR, HER2 and HER3 protein expression, relative to vehicle-treated and untreated cells, however endogenous HER2 was more resistant to coibamide A inhibition (Fig. 4A and B). HER3 expression was suppressed and the mature protein eliminated after exposure to only 10 nM coibamide A, whereas HER2 was detected at 10-fold higher coibamide A concentrations (Fig. 4A and B). To determine if coibamide A promotes proteasomal degradation of native HER proteins as a consequence of Sec61 inhibition, cells were treated with coibamide A (100 nM) in the presence, and absence, of the proteasome inhibitor bortezomib (25 nM). Immunoblot analysis of lysates prepared from co-treated cells showed the rescue of endogenous HER3, under these conditions (Fig. 4C and D), consistent with the pattern of degradation seen previously in response to synthetic cotransin molecules or the fungal natural product CAM741 [24,25]. In contrast, changes in endogenous EGFR and HER2 expression in response to co-treatment with bortezomib in BT-474 cells were not statistically significant (Fig. 4C and D).

To further understand the consequences of coibamide A-induced

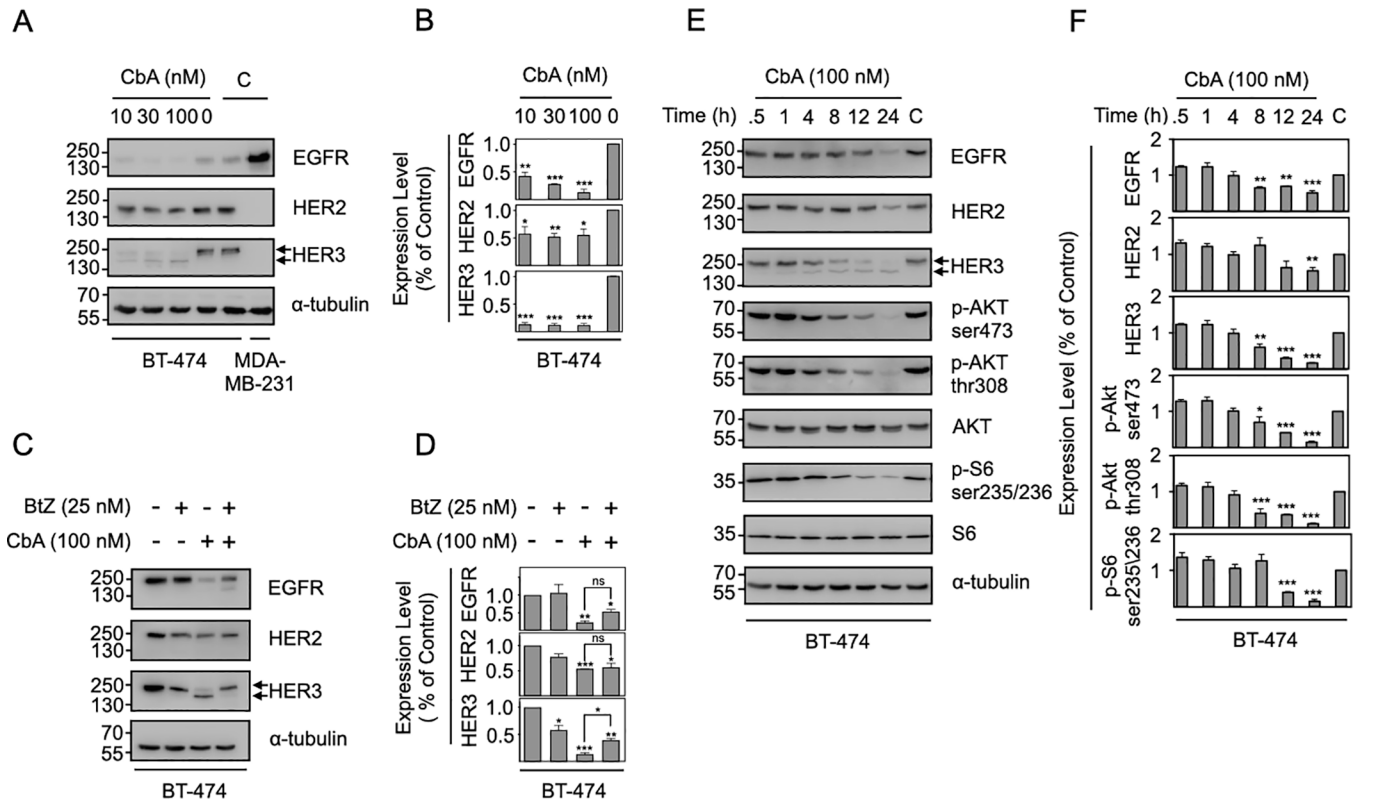

Fig. 4. HER family proteins show differential sensitivity to coibamide A. (A) Immunoblot analysis of EGFR, HER2, HER3 and α-tubulin expression in BT-474 treated with, or without (0.1% DMSO or untreated (C)), coibamide A ((CbA) 3 nM to 100 nM) for 24 h. Upper arrow represents the anticipated size of the mature form of HER3. (B) Quantification of immunoblot data shown in A from three independent experiments. Bars represent intensity of bands ± SE normalized to α-tubulin, relative to vehicle-treated cells (0). (C) CbA induces proteasomal-degradation of EGFR and HER3 in BT474 breast cancer cells. Immunoblot analysis of cells treated with vehicle (0.1% DMSO), CbA (100 nM), the proteasome inhibitor bortezomib (BtZ; 25 nM) or CbA and BtZ for 24 h. Cell lysates were probed simultaneously for EGFR, HER2, HER3 and α-tubulin. Images are representative of a comparison that was repeated at least three times with similar results. (D) Quantification of immunoblot data shown in C from three independent experiments. Bars represent intensity of bands ± SE normalized to α-tubulin, relative to vehicle-treated cells. (E) Time-dependent changes in the phosphorylation status of AKT and ribosomal S6 protein in response to coibamide A (CbA). HER2 positive BT474 cells were treated with, or without (0.1% DMSO), CbA (100 nM) for up to 24 h. Immunoblot analysis of EGFR, HER2, HER3, phospho-AKT(Ser473), phospho-AKT(Thr308), total AKT, phospho-S6(Ser235/236), total S6 and α-tubulin expression. (F) Quantification of immunoblot data shown in A from three independent experiments. Bars represent intensity of bands ± SE normalized to α-tubulin, relative to vehicle-treated cells (C). Statistical significance is indicated as: * $P < 0.01$, ** $P < 0.001$, *** $P < 0.0001$ or ns not significant.

suppression of HER family receptors, we evaluated the phosphorylation status of several key downstream elements of the HER signaling pathway downstream of the receptors. For these studies BT-474 cells were treated with coibamide A (100 nM) or 0.1% DMSO at various time points from 30 min to 24 h. Cell lysates were then analyzed for expression of AKT and S6 ribosomal protein, as well as EGFR, HER2 and HER3. In contrast to EGFR, HER2 and HER3, which showed statistically significant decreases in expression over time, we observed no significant changes in total AKT and total S6 ribosomal protein expression levels (Fig. 4E and F). BT474 lysates did, however, show dephosphorylation of AKT at Ser-473 and Thr-308, and dephosphorylation of S6 ribosomal protein at Ser-235/236 in response to coibamide A treatment (Fig. 4E and F). The observed changes in the phosphorylation status of AKT and S6 ribosomal protein were not evident as a rapid response to treatment but instead showed a steady decline that became statistically significant from 8 h to 24 h after treatment concomitant with the reduction in HER3 expression, a key activator of the Akt/PI3K pathway in BT474 cells. (Fig. 4E and F).

Given the partial response of HER2 to Sec61 inhibition, we selected this receptor for followup studies of HER2 cell surface expression using flow cytometry. Hormone-sensitive, HER2 positive MCF-7 cells were treated for 18 h with increasing concentrations of coibamide A (10 nM to 100 nM), 0.1% DMSO, or a control natural product inhibitor of ER-Golgi transport, brefeldin A (5 μM). After treatment, cells were stained with a phycoethrin-conjugated anti-HER2 antibody and samples analyzed by flow cytometry. Coibamide A induced a concentration-dependent decrease (red trace) in the fluorescence intensity of surface HER2 protein in MCF-7 cells, relative to control-treated (black trace) cells (Fig. 5A to C). Quantification of mean fluorescent intensity (MFI) revealed statistically significant decreases in HER2 expression that, at 100 nM coibamide A, was comparable to loss of surface HER2 expression induced by brefeldin A in viable cells (Fig. 5D and E). Thus, in order to compare the action of coibamide A relative to all four HER family members, each receptor was tagged with a C-terminal V5 epitope and transiently expressed in HEK293 cells (Fig. 6A). Studies of these cells, treated with or without coibamide A, revealed HER4 to be a coibamide-sensitive protein (Fig. 6B and C). Over-expressed HER2, was also sensitive and readily suppressed by coibamide A in these studies (Fig. 6B and C). Taken together, relative decreases in expression of the mature form of each HER protein, and differences in the ability of coibamide A to promote proteasomal degradation of HERs, indicate that endogenous HER proteins are differentially sensitive to Sec61 inhibition and raise the possibility of a coibamide-insensitive pool of HER2 in BT-474 breast cancer cells. Sec61-dependent inhibition of HER2 biosynthesis in MCF-7 cells, however, was sufficient to disrupt HER2 expression at the plasma membrane.

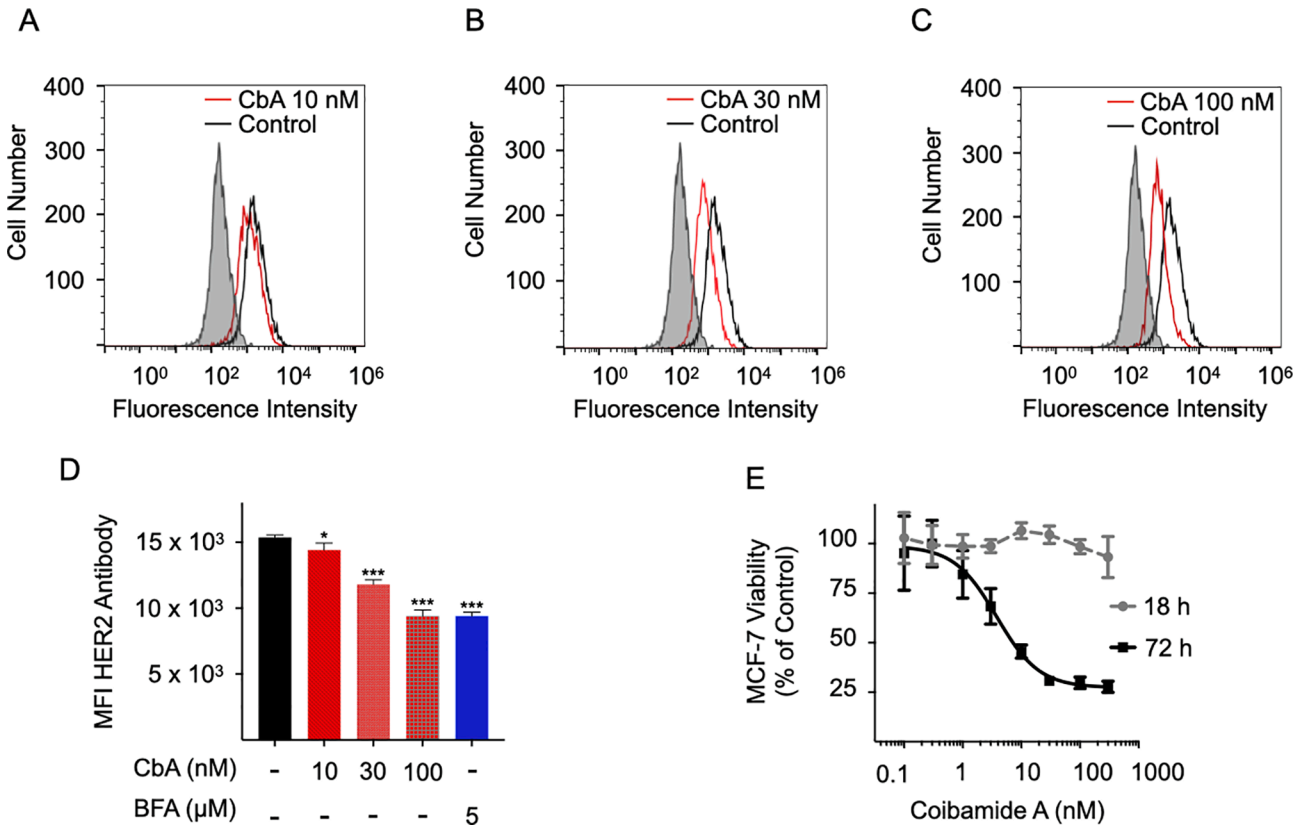

Fig. 5. Coibamide A decreases cell surface expression of HER2. (A to C) Flow cytometric analysis of HER2 fluorescence intensity in MCF-7 breast cancer cells treated with coibamide A (red line; 10 nM to 100 nM) or 0.1% DMSO (black line) for 18 h. Cells were harvested and stained with a PE-conjugated anti-human erbB2/HER-2 antibody (open profile) or isotype control antibody (shaded profile). (D) Quantification of Mean Fluorescent Intensity (MFI) in vehicle (0.1% DMSO) and coibamide A-treated MCF-7 cells in A to C relative to brefeldin A-treated control cells. Data is representative of an experiment that was repeated three times over the same concentration range; statistical significance is indicated as: * $P < 0.01$, *** $P < 0.0001$. (E) Viability of MCF-7 cells in the presence, and absence (0.1% DMSO), of coibamide A (0.1 nM to 300 nM) after 18 or 72 h. Data points show mean viability ± SE (n = 3 wells per treatment), relative to vehicle-treated cells, from a comparison that was repeated three times. (For interpretation of the references to colour in this figure legend, the reader is referred to the web version of this article.)

3.3. The HER3 signal peptide contributes to HER3 suppression by coibamide A

It has been shown that sensitivity of HER3 to the cotransin analogue CT8 is, like other synthetic and natural derivatives of HUN-7293 [24,62], critically dependent on identity of specific residues within the central hydrophobic region of the HER3 signal sequence [22]. To determine if coibamide A might also disrupt the signal sequence recognition of nascent HER3 by Sec61, we transiently expressed wild type HER3, or the CT8-resistant G11L/S15L signal peptide mutant in HEK293 cells (Fig. 7A) and exposed the transfected cells to increasing concentrations of coibamide A (0.3 nM to 10 nM) or vehicle (0.1% DMSO) for up to 24 hrs. As shown in Fig. 7B, coibamide A induced a clear concentration-dependent decrease in both HER3 and HER3(G11L/S15L) expression relative to vehicle-treated cells expressing the corresponding HER constructs. However, in side-by-side comparisons, the CT8-insenstive mutant HER3(G11L/S15L), was more resistant to lower concentrations of coibamide A (Fig. 7B). Statistically significant differences in expression of wild-type HER3 versus HER3(G11L/S15L) were observed at 3.0 nM coibamide A, whereas 10 nM coibamide was a fully effective inhibitor of HER3 and HER3(G11L/S15L) expression (Fig. 7B and C).

To determine if the observed responses were specific to coibamide A, we compared the action of apratoxin A on both endogenous and over-expressed HER proteins. Immunoblot analysis of cell lysates harvested from BT-474 cells treated with increasing concentrations of apratoxin A (1 nM to 100 nM), or vehicle (0.1% DMSO), showed a concentration-dependent reduction of EGFR, HER2 and HER3 expression by 24 h (Fig. 8A). This pattern was the same as that observed with coibamide A (Fig. 4A and B); apratoxin A produced statistically significant decreases in the expression of all three endogenous HER family proteins in BT474 cells with differences in relative sensitivity. Quantification of these results showed that HER3 expression was largely eliminated by apratoxin A, while HER2 was more resistant over the same concentration range (Fig. 8B). This similarity led us to ask if apratoxin A also interferes with HER3 biosynthesis at the level of the HER3 signal peptide. HER3 or HER3(G11L/S15L) proteins were transiently expressed in HEK293 cells and the cells exposed to coibamide A (3 nM), apratoxin A (3 nM) or vehicle (0.1% DMSO). Expression of the mature HER3 protein was strongly inhibited by coibamide A and apratoxin A (Fig. 8C and D), whereas HER3(G11L/S15L) was more resistant to coibamide A (Fig. 8C and D). Apratoxin A followed a similar trend although differences between wild-type and mutant were not significant (Fig. 8C and D). Collectively, these data suggest that the ER-targeting signal peptide does contribute to inhibtion of secretory protein biogenesis by coibamide A, whereas previously these compounds were assumed to be exclusively substrate-nonselective inhibitors of Sec61.

3.4. Cobamide A is a potent inhibitor of EGFR signaling in lung cancer cells

As the activity of EGFR is particularly relevant to non-small cell lung cancers which frequently harbor drug-resistant EGFR mutations [8], we extended our analysis to include lung cancer cell types with known aberrant signaling. Human PC-9 lung cancer cells (with a 15 base pair *EGFR* deletion E746-A750) or 11–18 cells (which harbor an activating

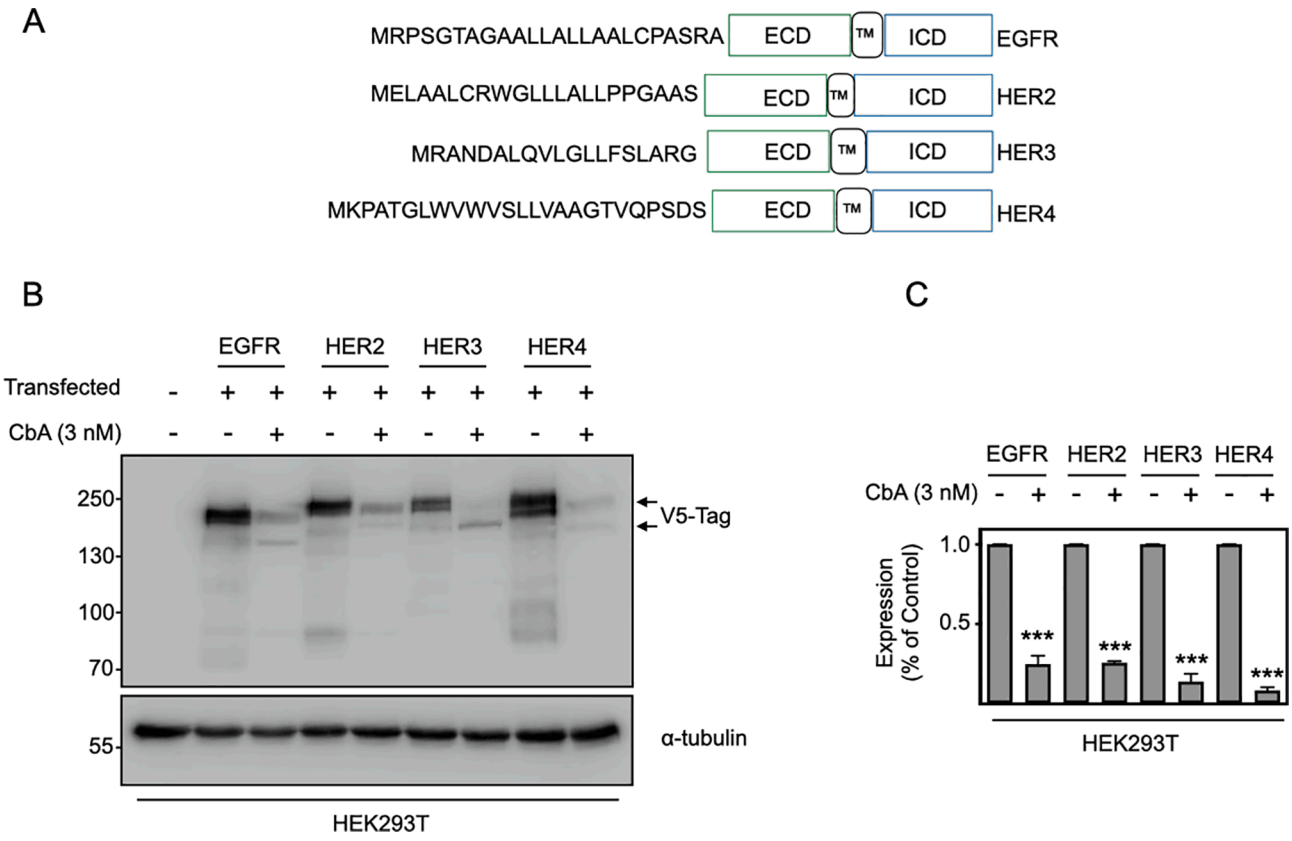

Fig. 6. Coibamide A suppresses expression of HER4. (A) Schematic representation of HER family members with extracellular (ECD), transmembrane (TM) and intracellular (ICD) domains shown. (B) Immunoblot analysis of HER family proteins transiently over-expressed in HEK293T cells and treated with, or without (0.1% DMSO) or CbA (3 nM). Cells were transfected with a pcDNA-DEST40 vector containing open reading frames of EGFR, HER2, HER3, or HER4 in-frame with a C-terminal V5 epitope. Cell lysates were harvested 24 h after treatment for immunoblot analysis with anti-V5 and anti-α-tubulin antibodies. Upper arrow represents the anticipated size of the mature form of HER3. (C) Quantification of immunoblot data shown in B from three independent experiments. Bars represent intensity of bands ± SE normalized to α-tubulin, relative to vehicle-treated cells (0). Statistical significance is indicated as *** $P < 0.0001$.

L858R mutation) were treated with coibamide A (1 to 100 nM), or vehicle (0.1% DMSO) for 24 h and the lysates harvested for immunoblot analysis. These mutations did not change the ability of the anti-EGFR antibody to detect the protein, however, mutant EGFR expression was reduced significantly in response to coibamide A treatment (Fig. 9A and B). In side-by-side evaluations of MDA-MB-231 breast cancer cells, 11–18 cells and PC-9 lung cancer cells, we observed a common pattern in response to treatment with coibamide A. All cell lysates showed statistically significant dephosphorylation of AKT at Ser-473 and Thr-308, dephosphorylation of S6 ribosomal protein at Ser-235/236 and, except in MDA-MB-231 cells, dephosphorylation of MAPK at Thr-202/Tyr-204 in response to coibamide A treatment (Fig. 9C and D).

Although technically challenging due to the ease in which coibamide A induces detachment of some adherent cell types from culture dishes over hours of exposure ([51,54] and Fig. 3C), we determined that the action of coibamide A on EGFR in PC-9 cells was also reversible at lower (1 nM) concentrations. Endogenous EGFR showed time-dependent re-expression (from 4 to 24 h) when coibamide A was diluted to sub-nanomolar final concentrations by the addition of fresh medium to culture dishes. Fig. 9E and F illustrate the recovery of EGFR expression in PC-9 cells following a 6-fold dilution from 1 nM to < 0.15 nM coibamide A. Similarly, 11–18 cells were sensitive to detachment with the combination of coibamide A plus bortezomib. Thus, in contrast to HER3 expression in BT474 breast cancer cells (Fig. 4C and D), EGFR expression showed no statistically significant recovery when 11–18 cells were treated with coibamide A (1 nM) in the presence of bortezomib (35 nM) (Fig. 9G and H).

3.5. Coibamide A potentiates the cytotoxic efficacy of small molecule kinase inhibitors

The potential for coibamide A to modify the efficacy of two well characterized kinase inhibitors was evaluated by testing coibamide A in combination with lapatinib or erlotinib in breast and lung cancer cells, respectively. Representative cell types showed distinct patterns of sensitivity to lapatinib or erlotinib when administered as single agents, reflecting a level of anticipated heterogeneity in response to these drugs [63]. BT-474 breast cancer cells were relatively sensitive to lapatinib alone (Fig. 10A), with an EC_{50} value of 8.9 ± 5.6 nM, whereas MDA-MB-468 breast cancer cells remained greater than 60% viable at the highest lapatinib (100 μM) concentration tested (Fig. 10B). Similarly, PC-9 lung cancer cells showed clear concentration-dependent sensitivity to erlotinib alone (Fig. 10C), EC_{50} = 8.4 ± 4.3 nM whereas 11–18 lung cancer cells remained 90% viable in the presence of 300 nM erlotinib and essentially resistant (Fig. 10D). When administered in combination with a kinase inhibitor, coibamide A (1 nM to 30 nM) induced a concentration-dependent reduction in the viability of BT-474 or PC-9 cancer cells treated with lapatinib (Fig. 10A) or erlotinib (Fig. 10C), respectively. Specifically, coibamide A potentiated the action of low concentrations of lapatinib (≤1 nM) or erlotinib (≤1 nM), resulting in enhanced cytotoxic efficacy of these kinase inhibitors against cultured BT-474 and PC-9 cells, respectively. Potentiation of the effect of lapatinib (≤0.1 nM) was also observed in MDA-MB-468 breast cancer cells, with evidence of synergy with combination treatment; coibamide A (3 nM to 30 nM) plus lapatanib (3 nM to 300 nM) consistently induced a greater loss in MDA-MB-468 cell viability than lapatinib alone

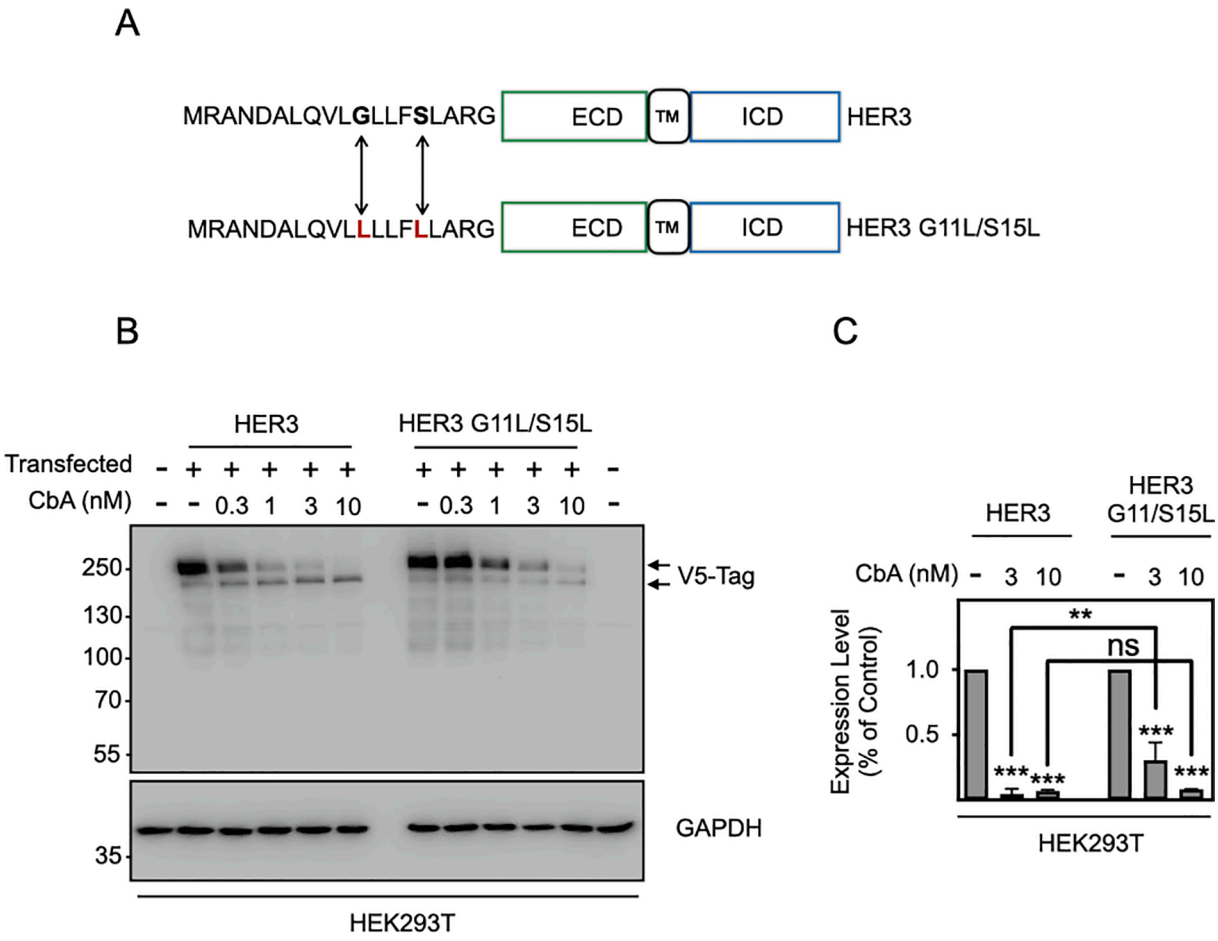

Fig. 7. The HER3 signal peptide contributes to coibamide A-induced block of HER3 expression. (A) Schematic representation of wild type HER3 and mutant HER3 (G11L/S15L) showing the location of mutations at sites 11 and 15 of the signal sequence where guanine and serine were replaced with lysine. (B) Immunoblot analysis of wild type HER3 and HER3(G11L/S15L) transiently over-expressed in HEK293T cells and treated with CbA (0.3 to 10 nM) or DMSO (0.1%). Cells were transfected with a pcDNA-DEST40 vector containing open reading frames of HER3 or HER3(G11L/S15L) in-frame with a C-terminal V5 epitope. Cell lysates were harvested 24 h after treatment for immunoblot analysis with anti-V5 and anti-GAPDH antibodies. Upper arrow represents the anticipated size of the mature form of HER3. (C) Quantification of immunoblot data for mature HER3 in response to 3 nM and 10 nM CbA in three independent experiments. Bars represent intensity of bands ± SE normalized to α-tubulin, relative to vehicle-treated cells (0). Statistical significance is indicated as: * $P < 0.01$, ** $P < 0.001$, *** $P < 0.0001$ or ns not significant.

(Fig. 10B). A clear decrease in cell viability was also observed when erlotinib (0.03 nM to 300 nM) was combined with coibamide A (30 nM) against 11–18 lung cancer cells (Fig. 10D). Further computational analysis of these pharmacological data for lapatinib-sensitive BT-474 cells (Fig. 10E), or erlotonib-sensitive PC-9 cells (Fig. 10F), predicted a pattern of synergy at multiple concentations when kinase inhibitors were co-administered with coibamide A.

4. Discussion

Natural products have served as a rich source of inspiration for drug development and in many cases these chemical entities are retained as important reference compounds for the biomedical research community [64,65]. Although at the stage of pre-clinical evaluation, the steady expansion of a relatively new class of natural product inhibitors of protein translocation into the ER secretory pathway is significant as these prototypes may help to define potential for selective suppression of specific Sec61 substrates as well as limitations in developing such compounds as future drugs [66,67]. Given that HER3 expression can be selectively blocked in HER2-amplified breast cancer cells with a pharmacological Sec61 inhibitor [22], the goal of the present study was to evaluate the action of broad-spectrum Sec61 inhibitors against members of the HER family of receptors. We determined that coibamide A and apratoxin A suppress HER3 protein expression with nanomolar potency and, in contrast to CT8, both compounds suppress expression of EGFR and HER4, whereas endogenous HER2 protein is effected to a lesser extent. Coibamide A promoted degradation of endogenous HER3 protein in cancer cells via a proteasome-dependent pathway and induced a steady decline in downstream markers of HER-mediated signaling consistent with a general loss of secretory function and therefore HER protein expression over hours of exposure. Concentration- and time-dependent decreases in EGFR expression in response to coibamide A were observed in triple-negative breast cancer and non-small cell lung cancer cells and were reversible, to an extent, in keeping with the general pharmacological properties of Sec61 inhibitors [24,68]. Our study complements previous work focused on translocon inhibitor selectivity and the biochemistry of cotranslational translocation [23–25], and demonstrates the general utility of Sec61 inhibitors to modulate expression of receptors that are already well-established therapeutic cancer targets. For example, a narrow-spectrum allosteric inhibitor of Sec61 function, such as CT8, blocks HER3 expression while inducing no significant change in the viability of HER2-amplified or other breast cancer cell types [22]. In contrast, and at the other end of the spectrum, coibamide A downregulates expression of all four HER family members, including EGFR in triple-negative breast cancer cells, and ultimately induces cell death as a function of concentration and time of exposure

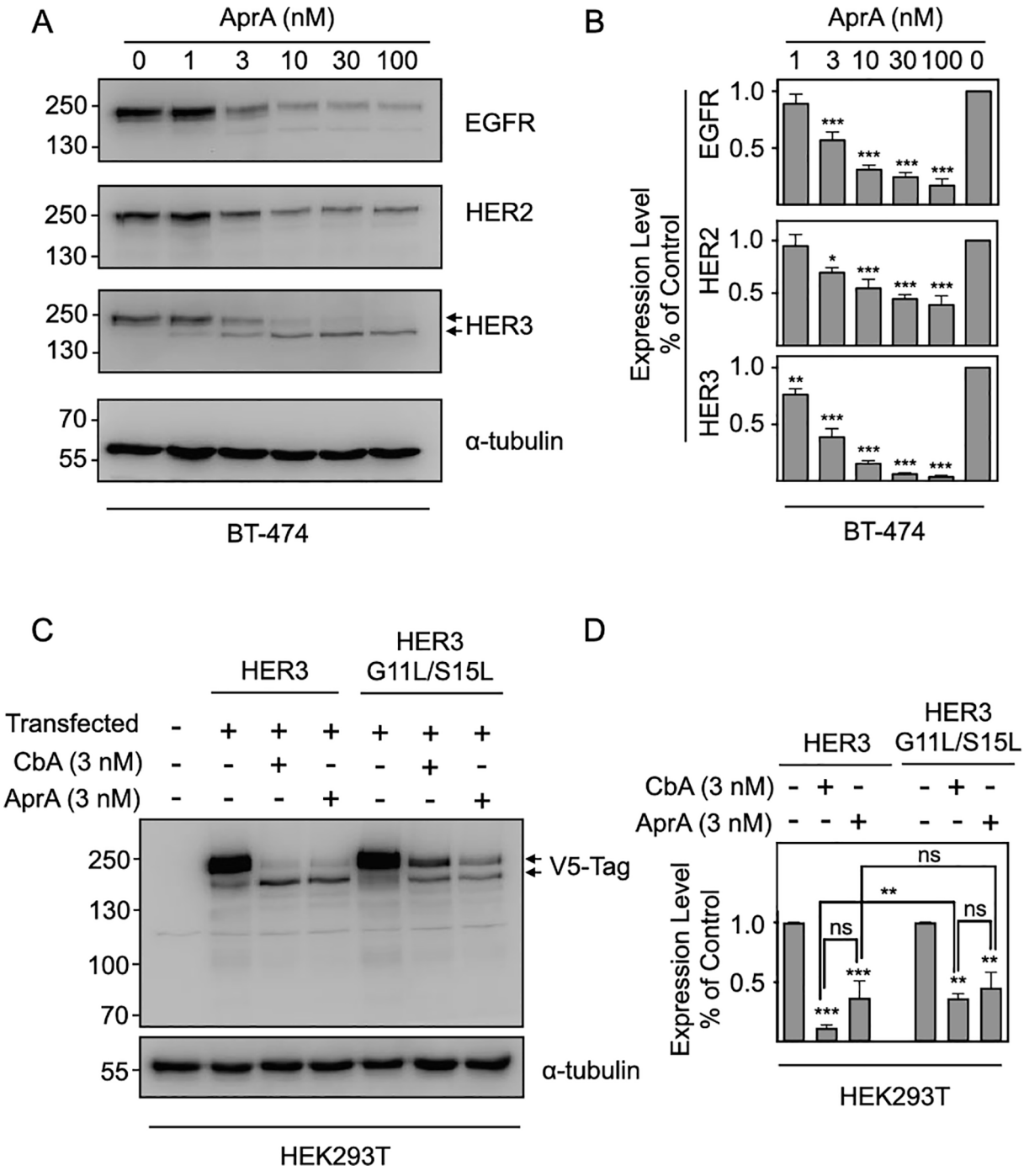

Fig. 8. HER family proteins show differential sensitivity to apratoxin A. (A) Immunoblot analysis of EGFR, HER2, HER3 and α-tubulin expression in BT-474 treated with, or without (0.1% DMSO), apratoxin A ((AprA) 1 nM to 100 nM) for 24 h. Upper arrow represents the anticipated size of the mature form of HER3. (B) Quantification of immunoblot data shown in A from three independent experiments. Bars represent intensity of bands ± SE normalized to α-tubulin, relative to vehicle-treated cells (0). (C) Immunoblot analysis of wild type HER3 and HER3(G11L/S15L) transiently expressed in HEK293T cells and treated with, or without (0.1% DMSO), CbA (3 nM) or AprA (3 nM). Cells were transfected with a pcDNA-DEST40 vector containing open reading frames of HER3 or HER3(G11L/S15L) in-frame with a C-terminal V5 epitope. Cell lysates were harvested 24 h after treatment for immunoblot analysis with anti-V5 and anti-α-tubulin antibodies. (D) Quantification of immunoblot data shown in C from three independent experiments. Bars represent intensity of bands ± SE normalized to α-tubulin, relative to vehicle-treated cells (0). Statistical significance is indicated as: * $P < 0.01$, ** $P < 0.001$, *** $P < 0.0001$ or ns not significant.

[49,50,54].

Although the full extent to which apratoxin A and coibamide A block protein translocation into the ER is not yet known, previous studies have shown the natural apratoxins inhibit expression of multiple RTKs in cancer cells with lead synthetic analogues displaying differential and cell-type specific effects [68–70]. In the present study, the pattern of HER sensitivity to coibamide A was confirmed to be the same as that of apratoxin A suggesting that both cyclic depsipeptides exert a similar response in cells. It was surprising however, that endogenous HER2 was partially resistant to coibamide A or apratoxin A treatment relative to other HER family members when compared over the same concentration range. The four individual HER proteins have distinct functional properties yet show a high level of structural homology; each is a type I integral membrane protein with a cleavable N-terminal signal peptide

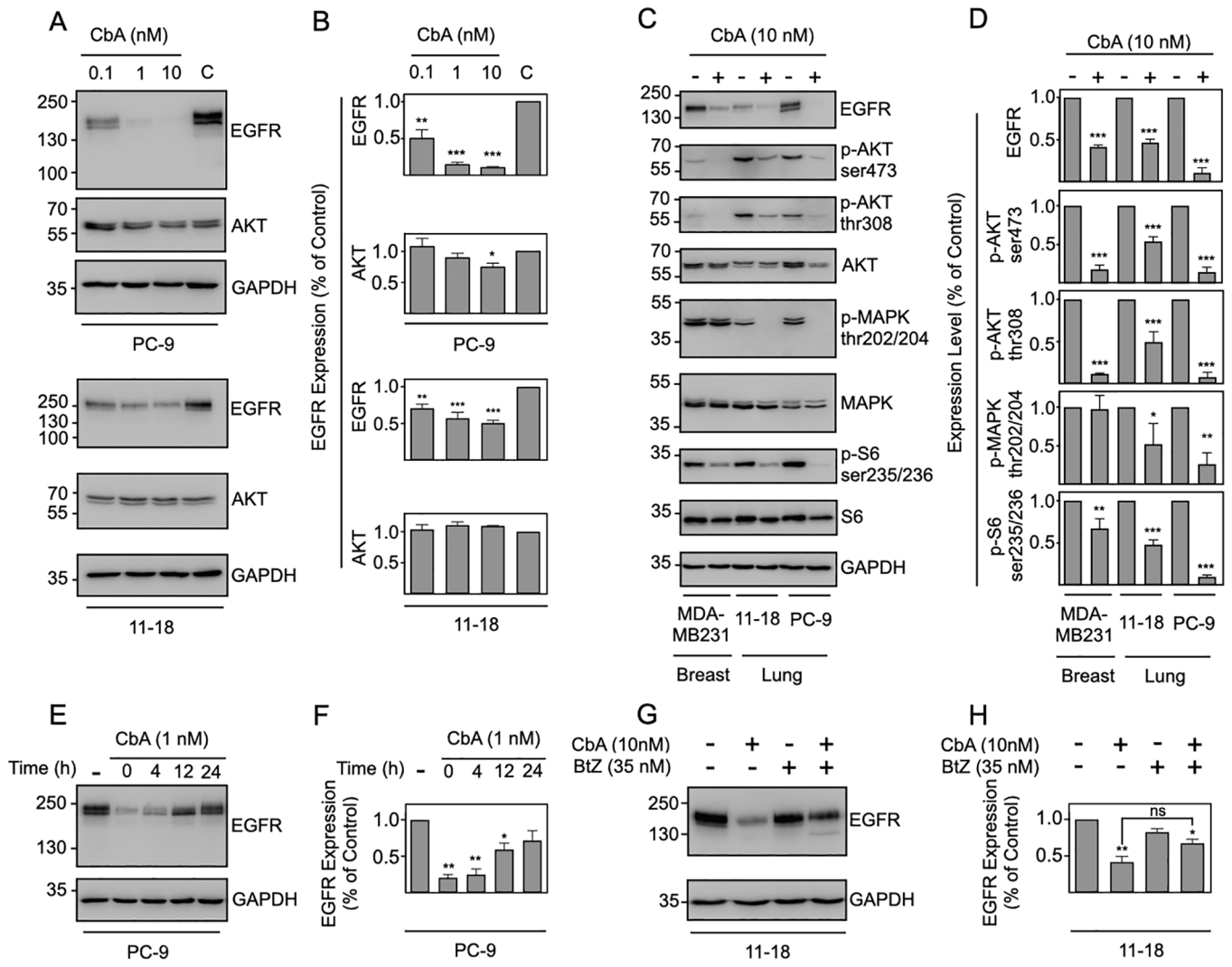

Fig. 9. Coibamide A is a reversible inhibitor of EGFR in lung cancer cells. (A) Immunoblot analysis of EGFR, AKT and GAPDH expression in PC-9 lung cancer cells treated with, or without (0.1% DMSO (C)), coibamide A ((CbA) 0.1 nM to 10 nM) for 24 h. (B) Quantification of immunoblot data shown in A from three independent experiments. Bars represent intensity of bands ± SE normalized to GAPDH, relative to vehicle-treated cells (C). (C) Comparison of the phosphorylation status of AKT, MAPK and ribosomal S6 protein in MDA-MB-231 breast, 11–18 and PC-9 lung cancer cells in response to coibamide A (CbA). Cells were treated with CbA (10 nM) or 0.1% DMSO for 24 h. Immunoblot analysis of EGFR, phospho-AKT(Ser473), phospho-AKT(Thr308), total AKT, phospho-MAPK (THr202/Tyr204), total MAPK, phospho-S6(235/236), total S6 and GAPDH expression. (D) Quantification of immunoblot data shown in C from three independent experiments. Bars represent intensity of bands ± SE normalized to GAPDH, relative to vehicle-treated cells. (E) Effect of coibamide A is reversible. PC-9 lung cancer cells were treated with, or without (0.1% DMSO), coibamide A (1 nM) for 24 h, the cell culture medium was then diluted with compound-free medium and cells harvested at the time of washout (0) or 4, 12 and 24 h later. PC-9 cell lysates were probed for EGFR and GAPDH. (F) Quantification of immunoblot data shown in E from three independent washout experiments. Bars represent intensity of bands ± SE normalized to GAPDH, relative to vehicle-treated cells. (G) CbA induces proteasomal-degradation of EGFR in 11–18 lung cancer cells. Immunoblot analysis of cells treated with vehicle (0.1% DMSO), CbA (1 nM), the proteasome inhibitor bortezomib (BtZ; 35 nM) or CbA and BtZ for 24 h. Cell lysates were probed simultaneously for EGFR and GAPDH. (H) Quantification of immunoblot data shown in panel H from three independent BtZ rescue experiments. Bars represent intensity of bands ± SE normalized to GAPDH, relative to vehicle-treated cells (-). Statistical significance is indicated as: * $P < 0.01$, ** $P < 0.001$, *** $P < 0.0001$ or ns not significant.

[71]. Biochemical assays with *in vitro* translated proteins have confirmed that both apratoxin A and coibamide A inhibit cotranslational translocation of representative secreted and integral membrane proteins including examples of type I proteins [47,52]. Our data complement these results and suggest that related type I proteins, even within the same family, are not equally affected by a broad-acting Sec61 inhibitor in a cellular context. As apparent differences in HER sensitivity could be influenced by multiple factors, further studies will be required to determine if the mechanistic basis for this effect is pharmacological and/or physiological in nature. It is conceivable that some nascent polypeptides are processed via alternate mechanisms that evade inhibitor block completely or, in the case of HER2, show only a partial response to coibamide or apratoxin treatment. Notably, coibamide A treatment resulted in a significant loss of cell surface HER2, suggesting that molecules that induce partial inhibition of a target substrate can have functional relevance. Studies of the mechanism of action of substrate-selective Sec61 inhibitors provide a useful comparison in this regard as, by definition, these compounds block biosynthesis of a limited number of Sec61 substrates. For example, the macrocyclic small molecule cyclotriazadisulfonamide (CADA) selectively inhibits cotranslational translocation of cell-surface cluster of differentiation 4 (CD4) by direct interaction with the CD4 signal peptide [72]. CADA is also described as a weak ER translocation inhibitor of sortilin resulting in partial down regulation of sortilin expression to approximately 50% of control [73]. Inhibitor concentration has been raised as a critical determinant of the selectivity of other substrate-selective Sec61

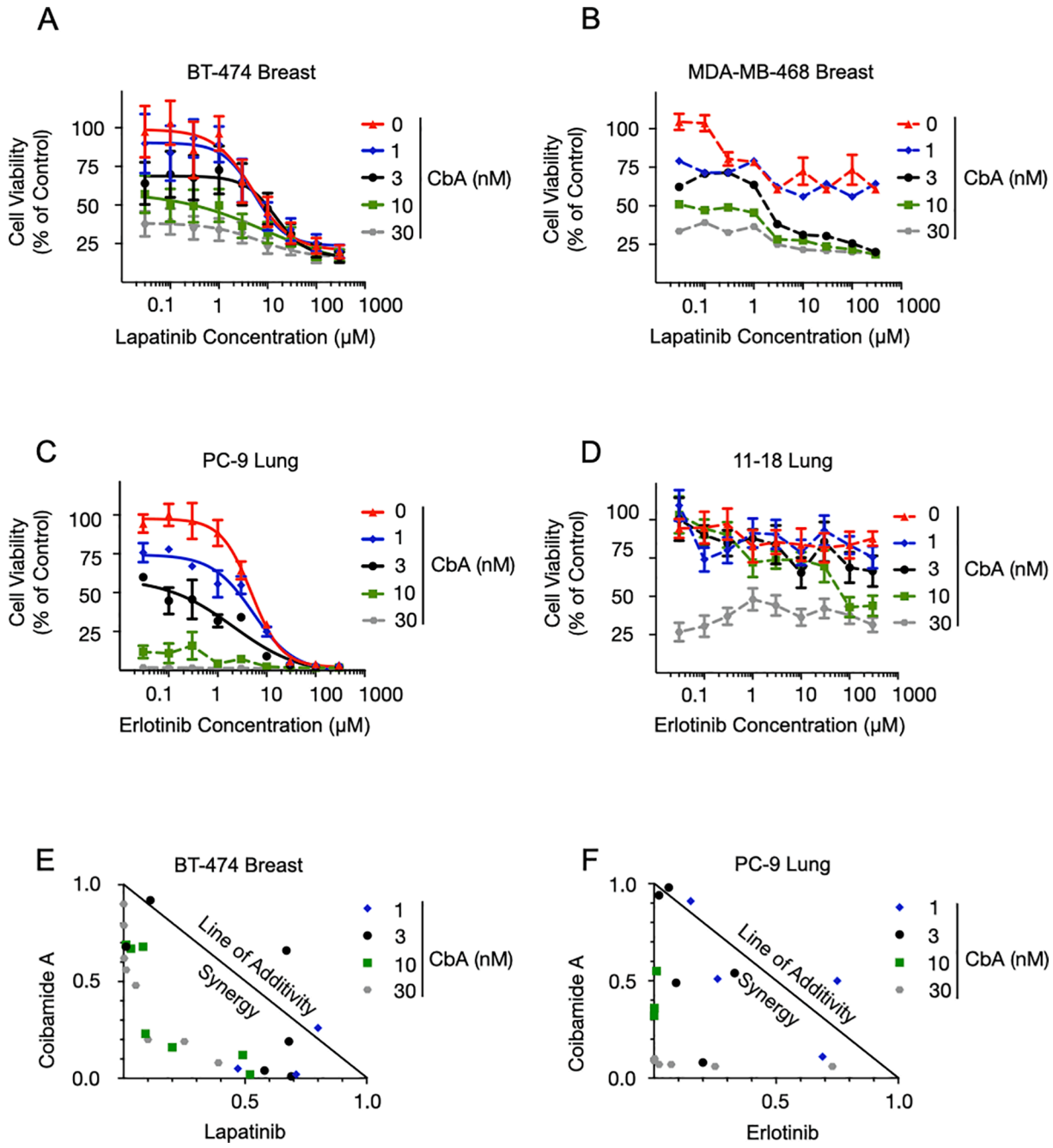

Fig. 10. Coibamide A enhances the cytotoxic efficacy of small molecule kinase inhibitors in combination treatment. (A and B) Concentration-response analysis of the effect of Lapatanib (3 nM to 300 nM) on breast (BT-474 and MDA-MD-468) cancer cells and (C and D) Erlotinib (3 nM to 300 nM) on lung (PC-9 and 11–18) cancer cells either alone (red line) or in combination with a fixed concentration of coibamide A (1 nM, 3 nM, 10 nM or 30 nM as indicated). Cells were exposed to kinase inhibitors, kinase inhibitors plus coibamide A, or vehicle (0.1% DMSO), for 72 h and cell viability determined using a Cell-Titer Glo® luminescent assay. Concentration-response curves are representative of three independent experiments for each drug combination. (E and F) Normalized isobolograms for coibamide A and lapatinib, or coibamide A and erlotonib, for non-constant ratio treatments shown in panel A (BT-474 cells) and panel C (PC-9 cells). Points located below the line of additivity confirm synergy between coibamide A and the kinase inhibitor. Isobolograms were generated using CompuSyn software. (For interpretation of the references to colour in this figure legend, the reader is referred to the web version of this article.)

inhibitors such as the cotransins in that inhibition of the biosynthesis of specific substrates is observed at nanomolar concentrations [23–25]. However, with stable isotopic labelling by amino acids in cell culture (SILAC), for a quantitative proteomic analysis of human HEPG2 hepatocellular carcinoma cells, cotransin was found to be less selective for secreted proteins at saturating (30 μM) concentrations [74]. Notably, although cotransin inhibited a greater percentage of the HEPG2 secretome at this high (30 μM) concentration, most integral membrane proteins remained cotransin-resistant revealing a level of complexity that had not previously been appreciated for these types of inhibitor-Sec61 protein interactions [74]. In the present study, we did not exceed 100 nM coibamide A and thus HER2 expression was likely not studied under steady state conditions. In addition, variations in the flux of individual Sec61 substrates through the secretory pathway are also likely to impact that ability to assess the full extent of a co-translational translocation block where the dynamics of individual protein transit and turnover in cells should also be taken into account.

Like CT8 [22],coibamide A and apratoxin A effectively suppressed

HER3 protein expression but likely do so via a subtly different mechanism. The Sec61 translocon is a heteromeric protein complex comprised of alpha, beta and gamma subunits with the largest alpha subunit forming the central pore of the channel. CT8, coibamide A and apratoxin A bind directly to the Sec61 alpha subunit at partially overlapping, but not identical, sites [40,52]. In the presence of CT8, some specific signal peptides are not correctly recognized by the Sec61 complex and thus the channel fails to open [24,39,67]. However, residues in the N-terminal HER3 signal peptide (G11 and S15), that are necessary and sufficient to confer full sensitivity to CT8 [22], had a relatively mild effect on HER3 sensitivity to either coibamide A or apratoxin A and only at low nanomolar concentrations. Residues G11 and S15 had no effect on the ability of either compound to block HER3 expression at higher concentrations. These findings underscore the general importance of assessing the cellular consequences of Sec61 inhibition over a range of concentrations and indicate that, in this assay, coibamide A and apratoxin A are more similar in action to each other, than either compound is to CT8. Furthermore, as with other Sec61 inhibitors [23,66,74],coibamide- or apratoxin-induced block of HER3 expression is likely not determined by an interaction with the signal peptide alone. Previous cell-free studies in which crosslinking reagents were employed to analyze the translocation of tissue necrosis factor alpha (TNFα) in the presence and absence of apratoxin A, or CT8, indicate that apratoxin A blocks an earlier step in nascent TNFα protein translocation than CT8 [23,39,47]. As multiple sequential steps are required for cotranslational translocation of proteins into the ER, a block in any of these steps (early or late) may have similar consequences in cells [66]. Thus, our results suggest that HER3 is an example of a Sec61 substrate that is vulnerable to both narrow- and broad-spectrum Sec61 inhibitors.

The ability of coibamide A and apratoxin A to decrease EGFR expression in breast and lung cancer cell types provides an attractive pharmacological opportunity as EGFR is an oncogenic driver that is frequently amplified or mutated in many other human cancers associated with treatment resistance such as forms of high-grade glioblastoma, head and neck squamous cell carcinoma and colorectal cancers [9,18]. Our results indicate that coibamide A inhibits EGFR expression and promotes degradation of EGFR via a proteasome-dependent pathway. However, in contrast to previous studies of cotransin-induced degradation of specific Sec61 substrates [22,24], the rescue of EGFR in cells co-treated with coibamide A plus bortezomib was not complete suggesting the loss of EGFR to a bortezomib-insensitive pathway. It has been proposed that a synthetic apratoxin analogue induces lysosomal degradation of EGFR via chaperone-mediated autophagy [75]. This selective form of autophagy can be distinguished from other catabolic pathways and typically removes soluble proteins from the cytosol [76]. As coibamide A and apratoxin A are strong inducers of macroautophagy [51,54], it is possible that acute block in co-translational translocation by a relatively nonselective Sec61 inhibitor diverts nascent unfolded proteins that fail to enter the secretory pathway to lysosomal degradation pathways as well as the ubiquitin–proteasome system. Taken together, these findings provide a framework for further interrogation of the coibamide structure–activity relationship to understand why triple-negative breast cancer and glioblastoma cell types are particularly sensitive to this natural product [49,50,54]. In addition to inhibiting EGFR expression in cell types representing difficult-to-treat cancers, coibamide A disrupts cellular proteostasis and induces both apoptotic and non-apoptotic forms of cell death [50,51,54]. As inspiration for future development of natural Sec61 inhibitors as drug leads, it is also encouraging that the coibamide A molecular structure appears amenable to simplification while retaining potent anti-tumor activity in mice [77]. In contrast to early in vivo studies with natural coibamide A inhibition of flank tumor growth was observed with poor therapeutic index [50],a synthetic coibamide analogue, [MAla3-MeAla6]-coibamide, was active against MDA-MB-231 breast cancer xenografts without inducing weight loss in tumor-bearing mice [77].

Coibamide A enhanced the cytotoxic efficacy of lapatinib or erlotinib in representative HER2-amplified breast (BT-474) and non-small cell lung (PC-9) cancer cells, respectively, but was also effective against EGFR positive, triple negative breast (MDA-MB-468) and EGFR mutant, non-small cell lung [11–18] cancer cell types that were relatively resistant to these specific kinase inhibitors. Lapatinib and erlotinib were selected as examples of clinically-relevant drugs approved for breast and non-small cell lung cancers, respectively [18], and although many other EGFR- and HER2-targeting drugs are in clinical use, our data illustrate the potential utility of a Sec61 inhibitor in combination with an established drug or when drug resistance is anticipated. Moreover, the complexity of HER signaling and inter-connectivity between receptors presents challenges with many of the established HER-targeting medicines and illustrates the need for new strategies [18]. For example, in addition to each receptor acting as a homodimer, EGFR forms a functional heterodimeric complex with HER2 and in this configuration has distinct downstream signaling activity [78–80]. Although HER2 was the least sensitive of the HER family members to coibamide A or apratoxin A, both natural products potently inhibited expression of all three HER2 dimerization partners and therefore could presumably impair the ability of HER2 to form a functional heterodimeric complex with EGFR, HER3 or HER4. These results complement previous findings with the selective Sec61 inhibitor CT8, in that the CT8-induced elimination of HER3 biosynthesis in HER2-amplified breast cancer cells was sufficient to dramatically attenuate signaling attributed to HER2-HER3 heterodimers and enhance the efficacy of lapatinib [22].

To date, all the natural products that have been identified as inhibitors of protein import into the ER bind to a similar region of the alpha subunit of Sec61 but are capable of transducing different cellular effects [40]. The potential for distinct pharmacological profiles arising from non-identical binding to Sec61 is supported by a recent comparison of the data sets available for coibamide A, apratoxin A and ipomoeassin F testing against the National Cancer Institute (NCI) 60 human tumor cell line panel [52]. Although all three cytotoxins are predicted to block co-translational translocation of a broad range of Sec61 client proteins, the extent to which compounds inhibit cancer cell growth is not identical [44,47,52]. This information, coupled with knowledge of Sec61 inhibitor preference for specific families of Sec61 client proteins, such as targeting of HERs and other RTK receptors by apratoxins and coibamide A [50,68,70,81], may inform future development of synthetic Sec61 inhibitors as cancer therapeutics.

Author contributions

SKaz, CEB, DRM, JDS and JEI designed and/or conducted the experiments. SKaw and SO designed and generated synthetic coibamide A. KLM isolated and purified natural product structures and verified assignment of synthetic coibamide A. SKaz, CEB, AR-S, MMM, BPD, VOP and JEI analyzed biological results and interpreted the data. SKaz and JEI wrote the original draft; SKaw, CEB, DRM, AR-S, JDS, MMM, BPD, VOP, SO and KLM reviewed and edited the manuscript.

Declaration of Competing Interest

The authors declare that they have no known competing financial interests or personal relationships that could have appeared to influence the work reported in this paper.

Acknowledgements

We thank Dylan Nelson of the High-Throughput Screening Services Laboratory at Oregon State University (OSU) for excellent technical assistance and Dr. Conroy Sun (OSU) for helpful discussions. This work was supported at an early stage by the American Brain Tumor Association (JEI), an NIH Fogarty International Center ICBG grant TW006634-06 (KLM), NIH/NCI R01CA122216 (MMM), the OSU College of Pharmacy and an American Foundation for Pharmaceutical Education

(AFPE) Pre-Doctoral Fellowship in the Pharmaceutical Sciences (JDS) and later by NIH/NIGMS R01GM132649 (VOP, SO, KLM, JEI) and NIH/NCCIH T32AT010131 (DRM). VOP is supported by Academy of Finland grants 289737, 314672 and 330255 and a grant from the Sigrid Juselius Foundation.

References

[1] M. Uhlen, L. Fagerberg, B.M. Hallstrom, C. Lindskog, P. Oksvold, A. Mardinoglu, A. Sivertsson, C. Kampf, E. Sjostedt, A. Asplund, I. Olsson, K. Edlund, E. Lundberg, S. Navani, C.A. Szigyarto, J. Odeberg, D. Djureinovic, J.O. Takanen, S. Hober, T. Alm, P.H. Edqvist, H. Berling, H. Tegel, J. Mulder, J. Rockberg, P. Nilsson, J. M. Schwenk, M. Hamsten, K. von Feilitzen, M. Forsberg, L. Persson, F. Johansson, M. Zwahlen, G. von Heijne, J. Nielsen, F. Ponten, Proteomics. Tissue-based map of the human proteome, Science 347 (6220) (2015) 1260419. Epub 2015/01/24. doi: 10.1126/science.1260419. PubMed PMID: 25613900.

[2] M.C. Lee, E.A. Miller, J. Goldberg, L. Orci, R. Schekman, Bi-directional protein transport between the ER and Golgi, Annu. Rev. Cell Dev. Biol. Epub 2004/10/12 (20) (2004) 87–123, https://doi.org/10.1146/annurev.cellbio.20.010403.105307. PubMed PMID: 15473836.

[3] J. Dudek, S. Pfeffer, P.-H. Lee, M. Jung, A. Cavalié, V. Helms, F. Förster, R. Zimmermann, Protein transport into the human endoplasmic reticulum, J. Mol. Biol. 427 (6) (2015) 1159–1175, https://doi.org/10.1016/j.jmb.2014.06.011.

[4] B.V.D. Berg, W.M. Clemons Jr, I. Collinson, Y. Modis, E. Hartmann, S.C. Harrison, T.A. Rapoport, X-ray structure of a protein-conducting channel, Nature 427 (6969) (2004) 36–44, https://doi.org/10.1038/nature02218.

[5] P.F. Egea, R.M. Stroud, Lateral opening of a translocon upon entry of protein suggests the mechanism of insertion into membranes, Proc. Natl. Acad. Sci. 107 (40) (2010) 17182–17187, https://doi.org/10.1073/pnas.1012556107.

[6] W.R. Critchley, C. Pellet-Many, B. Ringham-Terry, M.A. Harrison, I.C. Zachary, S. Ponnambalam, Receptor tyrosine kinase ubiquitination and de-ubiquitination in signal transduction and receptor trafficking, Cells 7 (3) (2018). Epub 2018/03/16. doi: 10.3390/cells7030022. PubMed PMID: 29543760; PMCID: PMC5870354.

[7] J. Schlessinger, Receptor tyrosine kinases: legacy of the first two decades, Cold Spring Harb. Perspect. Biol. 6 (3) (2014). Epub 2014/03/05. doi: 10.1101/cshperspect.a008912. PubMed PMID: 24591517; PMCID: PMC3949355.

[8] J. Baselga, Targeting tyrosine kinases in cancer: the second wave, Science 312 (5777) (2006) 1175–1178, https://doi.org/10.1126/science:1125951.

[9] Y. Yarden, G. Pines, The ERBB network: at last, cancer therapy meets systems biology, Nat. Rev. Cancer 12 (8) (2012) 553–563, https://doi.org/10.1038/nrc3309.

[10] F.J. Hendler, B.W. Ozanne, Human squamous cell lung cancers express increased epidermal growth factor receptors. J. Clin. Invest. 74 (2) (1984) 647–651, https://doi.org/10.1172/JCI111463.

[11] S.V. Sharma, D.W. Bell, J. Settleman, D.A. Haber, Epidermal growth factor receptor mutations in lung cancer, Nat. Rev. Cancer 7 (3) (2007) 169–181, https://doi.org/10.1038/nrc2088.

[12] T.A. Libermann, N. Razon, A.D. Bartal, Y. Yarden, J. Schlessinger, H. Soreq, Expression of epidermal growth factor receptors in human brain tumors, Cancer Res. 44 (2) (1984) 753–760. Epub 1984/02/01 PubMed PMID: 6318976.

[13] N. Sugawa, A.J. Ekstrand, C.D. James, V.P. Collins, Identical splicing of aberrant epidermal growth factor receptor transcripts from amplified rearranged genes in human glioblastomas. Proc. Natl. Acad. Sci. 87 (21) (1990) 8602–8606, https://doi.org/10.1073/pnas.87.21.8602.

[14] L. Frederick, X.Y. Wang, G. Eley, C.D. James, Diversity and frequency of epidermal growth factor receptor mutations in human glioblastomas, Cancer Res. 60 (5) (2000) 1383–1387. Epub 2000/03/23 PubMed PMID: 10728703.

[15] M.H. Kraus, N.C. Popescu, S.C. Amsbaugh, C.R. King, Overexpression of the EGF receptor-related proto-oncogene erbB-2 in human mammary tumor cell lines by different molecular mechanisms, EMBO J. 6 (3) (1987) 605–610, https://doi.org/10.1002/j.1460-2075.1987.tb04797.x.

[16] D.J. Slamon, G.M. Clark, S.G. Wong, W.J. Levin, A. Ullrich, W.L. McGuire, Human breast cancer: correlation of relapse and survival with amplification of the HER-2/neu oncogene, Science 235 (4785) (1987) 177–182. Epub 1987/01/09 PubMed PMID: 3798106.

[17] R. Bose, S.M. Kavuri, A.C. Searleman, W. Shen, D. Shen, D.C. Koboldt, J. Monsey, N. Goel, A.B. Aronson, S. Li, C.X. Ma, L.i. Ding, E.R. Mardis, M.J. Ellis, Activating HER2 mutations in HER2 gene amplification negative breast cancer, Cancer Discov. 3 (2) (2013) 224–237, https://doi.org/10.1158/2159-8290.CD-12-0349.

[18] C. Arteaga, J. Engelman, ERBB receptors: from oncogene discovery to basic science to mechanism-based cancer therapeutics, Cancer Cell 25 (3) (2014) 282–303, https://doi.org/10.1016/j.ccr.2014.02.025.

[19] A. Ruiz-Saenz, M.M. Moasser, Targeting HER2 by combination therapies, JCO 36 (8) (2018) 808–811, https://doi.org/10.1200/JCO.2017.77.1899.

[20] C. Holohan, S. Van Schaeybroeck, D.B. Longley, P.G. Johnston, Cancer drug resistance: an evolving paradigm, Nat. Rev. Cancer 13 (10) (2013) 714–726, https://doi.org/10.1038/nrc3599.

[21] N. Tebbutt, M.W. Pedersen, T.G. Johns, Targeting the ERBB family in cancer: couples therapy, Nat. Rev. Cancer 13 (9) (2013) 663–673, https://doi.org/10.1038/nrc3559.

[22] A. Ruiz-Saenz, M. Sandhu, Y. Carrasco, R.L. Maglathlin, J. Taunton, M.M. Moasser, Targeting HER3 by interfering with its Sec61-mediated cotranslational insertion into the endoplasmic reticulum, Oncogene 34 (41) (2015) 5288–5294, https://doi.org/10.1038/onc.2014.455.

[23] S.V. Maifeld, A.L. MacKinnon, J.L. Garrison, A. Sharma, E.J. Kunkel, R.S. Hegde, J. Taunton, Secretory protein profiling reveals TNF-alpha inactivation by selective and promiscuous Sec61 modulators, Chem. Biol. 18 (9) (2011) 1082–1088. Epub 2011/09/29. doi: 10.1016/j.chembiol.2011.06.015. PubMed PMID: 21944747; PMCID: PMC3855466.

[24] J.L. Garrison, E.J. Kunkel, R.S. Hegde, J. Taunton, A substrate-specific inhibitor of protein translocation into the endoplasmic reticulum, Nature 436 (7048) (2005) 285–289, https://doi.org/10.1038/nature03821.

[25] J. Besemer, H. Harant, S. Wang, B. Oberhauser, K. Marquardt, C.A. Foster, E. P. Schreiner, J.E. de Vries, C. Dascher-Nadel, I.J.D. Lindley, Selective inhibition of cotranslational translocation of vascular cell adhesion molecule 1, Nature 436 (7048) (2005) 290–293, https://doi.org/10.1038/nature03670.

[26] T. Holbro, R.R. Beerli, F. Maurer, M. Koziczak, C.F. Barbas, N.E. Hynes, The ErbB2/ErbB3 heterodimer functions as an oncogenic unit: ErbB2 requires ErbB3 to drive breast tumor cell proliferation, Proc. Natl. Acad. Sci. 100 (15) (2003) 8933–8938, https://doi.org/10.1073/pnas.1537685100.

[27] A.C. Hsieh, M.M. Moasser, Targeting HER proteins in cancer therapy and the role of the non-target HER3, Br. J. Cancer 97 (4) (2007) 453–457, https://doi.org/10.1038/sj.bjc.6603910.

[28] S.T. Lee-Hoeflich, L. Crocker, E. Yao, T. Pham, X. Munroe, K.P. Hoeflich, M. X. Sliwkowski, H.M. Stern, A central role for HER3 in HER2-amplified breast cancer: implications for targeted therapy, Cancer Res. 68 (14) (2008) 5878–5887, https://doi.org/10.1158/0008-5472.CAN-08-0380.

[29] S.P. Soltoff, K.L. Carraway 3rd, S.A. Prigent, W.G. Gullick, L.C. Cantley, ErbB3 is involved in activation of phosphatidylinositol 3-kinase by epidermal growth factor. Mol. Cell. Biol. 14 (6) (1994) 3550–3558, https://doi.org/10.1128/MCB.14.6.3550.

[30] S.A. Prigent, W.J. Gullick, Identification of c-erbB-3 binding sites for phosphatidylinositol 3′-kinase and SHC using an EGF receptor/c-erbB-3 chimera, EMBO J. 13 (12) (1994) 2831–2841, https://doi.org/10.1002/j.1460-2075.1994.tb06577.x.

[31] N.V. Sergina, M. Rausch, D. Wang, J. Blair, B. Hann, K.M. Shokat, M.M. Moasser, Escape from HER-family tyrosine kinase inhibitor therapy by the kinase-inactive HER3, Nature 445 (7126) (2007) 437–441, https://doi.org/10.1038/nature05474.

[32] N. Jura, Y. Shan, X. Cao, D.E. Shaw, J. Kuriyan, Structural analysis of the catalytically inactive kinase domain of the human EGF receptor 3, Proc. Natl. Acad. Sci. 106 (51) (2009) 21608–21613, https://doi.org/10.1073/pnas.0912101106.

[33] D.N. Amin, N. Sergina, D. Ahuja, M. McMahon, J.A. Blair, D. Wang, B. Hann, K. M. Koch, K.M. Shokat, M.M. Moasser, Resiliency and vulnerability in the HER2-HER3 tumorigenic driver, Sci. Transl. Med. 2 (16) (2010) 16ra7. Epub 2010/04/08. doi: 10.1126/scitranslmed.3000389. PubMed PMID: 20371474; PMCID: PMC3033659.

[34] J.T. Garrett, M.G. Olivares, C. Rinehart, N.D. Granja-Ingram, V. Sanchez, A. Chakrabarty, B. Dave, R.S. Cook, W. Pao, E. McKinely, H.C. Manning, J. Chang, C.L. Arteaga, Transcriptional and posttranslational up-regulation of HER3 (ErbB3) compensates for inhibition of the HER2 tyrosine kinase, Proc. Natl. Acad. Sci. 108 (12) (2011) 5021–5026, https://doi.org/10.1073/pnas.1016140108.

[35] Y. Chen, M. Bilban, C.A. Foster, D.L. Boger, Solution-phase parallel synthesis of a pharmacophore library of HUN-7293 analogues: a general chemical mutagenesis approach to defining structure-function properties of naturally occurring cyclic (depsi)peptides, J. Am. Chem. Soc. 124 (19) (2002) 5431–5440. Epub 2002/05/09 PubMed PMID: 11996584.

[36] C.A. Foster, M. Dreyfuss, B. Mandak, J.G. Meingassner, H.U. Naegeli, A. Nussbaumer, L. Oberer, G. Scheel, E.-M. Swoboda, Pharmacological modulation of endothelial cell-associated adhesion molecule expression: implications for future treatment of dermatological diseases, J. Dermatol. 21 (11) (1994) 847–854, https://doi.org/10.1111/j.1346-8138.1994.tb03300.x.

[37] U. Hommel, H.P. Weber, L. Oberer, H.U. Naegeli, B. Oberhauser, C.A. Foster, The 3D-structure of a natural inhibitor of cell adhesion molecule expression, FEBS Lett. 379 (1) (1996) 69–73. Epub 1996/01/22 PubMed PMID: 8566232.

[38] C. Westendorf, A. Schmidt, I. Coin, J. Furkert, I. Ridelis, D. Zampatis, C. Rutz, B. Wiesner, W. Rosenthal, M. Beyermann, R. Schülein, Inhibition of biosynthesis of human endothelin B receptor by the cyclodepsipeptide cotransin, J. Biol. Chem. 286 (41) (2011) 35588–35600, https://doi.org/10.1074/jbc.M111.239244.

[39] A.L. Mackinnon, V.O. Paavilainen, A. Sharma, R.S. Hegde, J. Taunton, An allosteric Sec61 inhibitor traps nascent transmembrane helices at the lateral gate, Elife 3 (2014) e01483. Epub 2014/02/06. doi: 10.7554/eLife.01483. PubMed PMID: 24497544; PMCID: PMC3913039.

[40] H. Luesch, V.O. Paavilainen, Natural products as modulators of eukaryotic protein secretion, Nat. Prod. Rep. 37 (5) (2020) 717–736, https://doi.org/10.1039/C9NP00066F.

[41] T. Junne, J. Wong, C. Studer, T. Aust, B.W. Bauer, M. Beibel, B. Bhullar, R. Bruccoleri, J. Eichenberger, D. Estoppey, N. Hartmann, B. Knapp, P. Krastel, N. Melin, E.J. Oakeley, L. Oberer, R. Riedl, G. Roma, S. Schuierer, F. Petersen, J. A. Tallarico, T.A. Rapoport, M. Spiess, D. Hoepfner, Decatransin, a new natural product inhibiting protein translocation at the Sec61/SecYEG translocon, J. Cell Sci. 128 (6) (2015) 1217–1229, https://doi.org/10.1242/jcs.165746.

[42] M. McKenna, R.E. Simmonds, S. High, Mechanistic insights into the inhibition of Sec61-dependent co- and post-translational translocation by mycolactone, J. Cell Sci. 129 (7) (2016) 1404–1415, https://doi.org/10.1242/jcs.182352.

[43] M. McKenna, R.E. Simmonds, S. High, Mycolactone reveals the substrate-driven complexity of Sec61-dependent transmembrane protein biogenesis, J. Cell Sci. 130 (7) (2017) 1307–1320, https://doi.org/10.1242/jcs.198655.

[44] G. Zong, Z. Hu, S. O'Keefe, D. Tranter, M.J. Iannotti, L. Baron, B. Hall, K. Corfield, A.O. Paatero, M.J. Henderson, P. Roboti, J. Zhou, X. Sun, M. Govindarajan, J. M. Rohde, N. Blanchard, R. Simmonds, J. Inglese, Y. Du, C. Demangel, S. High, V.

O. Paavilainen, W.Q. Shi, Ipomoeassin F binds Sec61alpha to inhibit protein translocation, J. Am. Chem. Soc. (2019). Epub 2019/05/07. doi: 10.1021/jacs.8b13506. PubMed PMID: 31059257.
[45] H. Luesch, W.Y. Yoshida, R.E. Moore, V.J. Paul, T.H. Corbett, Total structure determination of apratoxin A, a potent novel cytotoxin from the marine cyanobacterium lyngbyamajuscula, J. Am. Chem. Soc. 123 (23) (2001) 5418–5423, https://doi.org/10.1021/ja010453j.
[46] H. Luesch, S.K. Chanda, R.M. Raya, P.D. DeJesus, A.P. Orth, J.R. Walker, J. C. Izpisúa Belmonte, P.G. Schultz, A functional genomics approach to the mode of action of apratoxin A, Nat. Chem. Biol. 2 (3) (2006) 158–167, https://doi.org/10.1038/nchembio769.
[47] A. Paatero, J. Kellosalo, B. Dunyak, J. Almaliti, J. Gestwicki, W. Gerwick, J. Taunton, V. Paavilainen, Apratoxin kills cells by direct blockade of the sec61 protein translocation channel, Cell Chem. Biol. 23 (5) (2016) 561–566, https://doi.org/10.1016/j.chembiol.2016.04.008.
[48] K.-C. Huang, Z. Chen, Y. Jiang, S. Akare, D. Kolber-Simonds, K. Condon, S. Agoulnik, K. Tendyke, Y. Shen, K.-M. Wu, S. Mathieu, H.-W. Choi, X. Zhu, H. Shimizu, Y. Kotake, W.H. Gerwick, T. Uenaka, M. Woodall-Jappe, K. Nomoto, Apratoxin A shows novel pancreas-targeting activity through the binding of Sec 61, Mol. Cancer Ther. 15 (6) (2016) 1208–1216, https://doi.org/10.1158/1535-7163.MCT-15-0648.
[49] R.A. Medina, D.E. Goeger, P. Hills, S.L. Mooberry, N. Huang, L.I. Romero, E. Ortega-Barría, W.H. Gerwick, K.L. McPhail, Coibamide A, a potent antiproliferative cyclic depsipeptide from the panamanian marine cyanobacterium leptolyngbya sp. J. Am. Chem. Soc. 130 (20) (2008) 6324–6325, https://doi.org/10.1021/ja801383f.
[50] J.D. Serrill, X. Wan, A.M. Hau, H.S. Jang, D.J. Coleman, A.K. Indra, A.W.G. Alani, K.L. McPhail, J.E. Ishmael, Coibamide A, a natural lariat depsipeptide, inhibits VEGFA/VEGFR2 expression and suppresses tumor growth in glioblastoma xenografts, Invest. New Drugs 34 (1) (2016) 24–40, https://doi.org/10.1007/s10637-015-0303-x.
[51] X. Wan, J.D. Serrill, I.R. Humphreys, M. Tan, K.L. McPhail, I.G. Ganley, J. E. Ishmael, ATG5 promotes death signaling in response to the cyclic depsipeptides coibamide A and apratoxin A, Mar Drugs. 16 (3) (2018). Epub 2018/03/02. doi: 10.3390/md16030077. PubMed PMID: 29494533; PMCID: PMC5867621.
[52] D. Tranter, A.O. Paatero, S. Kawaguchi, S. Kazemi, J.D. Serrill, J. Kellosalo, W. K. Vogel, U. Richter, D.R. Mattos, X. Wan, C.C. Thornburg, S. Oishi, K.L. McPhail, J. E. Ishmael, V.O. Paavilainen, Coibamide A targets Sec61 to prevent biogenesis of secretory and membrane proteins, ACS Chem. Biol. 15 (8) (2020) 2125–2136, https://doi.org/10.1021/acschembio.0c00325.s001.
[53] C.C. Thornburg, E.S. Cowley, J. Sikorska, L.A. Shaala, J.E. Ishmael, D.T.A. Youssef, K.L. McPhail, Apratoxin H and apratoxin A sulfoxide from the red sea cyanobacterium moorea producens, J. Nat. Prod. 76 (9) (2013) 1781–1788, https://doi.org/10.1021/np4004992.
[54] A.M. Hau, J.A. Greenwood, C.V. Lohr, J.D. Serrill, P.J. Proteau, I.G. Ganley, K. L. McPhail, J.E. Ishmael, Coibamide A induces mTOR-independent autophagy and cell death in human glioblastoma cells, PloS One 8 (6) (2013). Epub 2013/06/14. doi: 10.1371/journal.pone.0065250. PubMed PMID: 23762328; PMCID: PMC3675158.
[55] T.-C. Chou, P. Talalay, Quantitative analysis of dose-effect relationships: the combined effects of multiple drugs or enzyme inhibitors, Adv. Enzyme Regul. 22 (1984) 27–55, https://doi.org/10.1016/0065-2571(84)90007-4.
[56] T.-C. Chou, Theoretical basis, experimental design, and computerized simulation of synergism and antagonism in drug combination studies, Pharmacol. Rev. 58 (3) (2006) 621–681, https://doi.org/10.1124/pr.58.3.10.
[57] C.E. Badr, J.W. Hewett, X.O. Breakefield, B.A. Tannous, A highly sensitive assay for monitoring the secretory pathway and ER stress, PloS One 2 (6) (2007). Epub 2007/06/28. doi: 10.1371/journal.pone.0000571. PubMed PMID: 17593970; PMCID: PMC1892804.
[58] W.D. Foulkes, I.E. Smith, J.S. Reis-Filho, Triple-negative breast cancer, N. Engl. J. Med. 363 (20) (2010) 1938–1948, https://doi.org/10.1056/NEJMra1001389.
[59] G. Yao, Z. Pan, C. Wu, W. Wang, L. Fang, W.u. Su, Efficient synthesis and stereochemical revision of coibamide A, J. Am. Chem. Soc. 137 (42) (2015) 13488–13491, https://doi.org/10.1021/jacs.5b09286.
[60] R. Nabika, T.L. Suyama, A.M. Hau, R. Misu, H. Ohno, J.E. Ishmael, K.L. McPhail, S. Oishi, N. Fujii, Synthesis and biological evaluation of the [d-MeAla11]-epimer of coibamide A, Bioorg. Med. Chem. Lett. 25 (2) (2015) 302–306, https://doi.org/10.1016/j.bmcl.2014.11.044.
[61] G.A. Sable, J. Park, H. Kim, S.-J. Lim, S. Jang, D. Lim, Solid-phase total synthesis of the proposed structure of coibamide a and its derivative: highly methylated cyclic depsipeptides: synthesis of putative coibamide A and derivative, Eur. J. Org. Chem. 2015 (32) (2015) 7043–7052, https://doi.org/10.1002/ejoc.201500697.
[62] H. Harant, N. Lettner, L. Hofer, B. Oberhauser, J.E. de Vries, I.J.D. Lindley, The translocation inhibitor CAM741 interferes with vascular cell adhesion molecule 1 signal peptide insertion at the translocon, J. Biol. Chem. 281 (41) (2006) 30492–30502, https://doi.org/10.1074/jbc.M607243200.
[63] C.R. Chong, P.A. Jänne, The quest to overcome resistance to EGFR-targeted therapies in cancer, Nat. Med. 19 (11) (2013) 1389–1400, https://doi.org/10.1038/nm.3388.
[64] Y.-W. Chin, M.J. Balunas, H.B. Chai, A.D. Kinghorn, Drug discovery from natural sources, AAPS J. 8 (2) (2006) E239–E253, https://doi.org/10.1007/BF02854894.
[65] D.J. Newman, G.M. Cragg, Natural products as sources of new drugs from 1981 to 2014, J. Nat. Prod. 79 (3) (2016) 629–661, https://doi.org/10.1021/acs.jnatprod.5b01055.s002.
[66] K.-U. Kalies, K. Römisch, Inhibitors of protein translocation across the ER membrane: ER protein translocation inhibitors, Traffic 16 (10) (2015) 1027–1038, https://doi.org/10.1111/tra.12308.
[67] V. Van Puyenbroeck, K. Vermeire, Inhibitors of protein translocation across membranes of the secretory pathway: novel antimicrobial and anticancer agents, Cell. Mol. Life Sci. 75 (9) (2018) 1541–1558, https://doi.org/10.1007/s00018-017-2743-2.
[68] Y. Liu, B.K. Law, H. Luesch, Apratoxin A reversibly inhibits the secretory pathway by preventing cotranslational translocation, Mol. Pharmacol. 76 (1) (2009) 91–104, https://doi.org/10.1124/mol.109.056085.
[69] Q.-Y. Chen, Y. Liu, W. Cai, H. Luesch, Improved total synthesis and biological evaluation of potent apratoxin s4 based anticancer agents with differential stability and further enhanced activity, J. Med. Chem. 57 (7) (2014) 3011–3029, https://doi.org/10.1021/jm4019965.
[70] W. Cai, Q.-Y. Chen, L.H. Dang, H. Luesch, Apratoxin S10, a dual inhibitor of angiogenesis and cancer cell growth to treat highly vascularized tumors, ACS Med. Chem. Lett. 8 (10) (2017) 1007–1012, https://doi.org/10.1021/acsmedchemlett.7b00192.s001.
[71] M.A. Lemmon, J. Schlessinger, K.M. Ferguson, The EGFR family: not so prototypical receptor tyrosine kinases, Cold Spring Harb. Perspect. Biol. 6 (4) (2014). Epub 2014/04/03. doi: 10.1101/cshperspect.a020768. PubMed PMID: 24691965; PMCID: PMC3970421.
[72] K. Vermeire, T.W. Bell, V. Van Puyenbroeck, A. Giraut, S. Noppen, S. Liekens, D. Schols, E. Hartmann, K.U. Kalies, M. Marsh, Signal peptide-binding drug as a selective inhibitor of co-translational protein translocation, PLoS Biol. 12 (12) (2014). Epub 2014/12/03. doi: 10.1371/journal.pbio.1002011. PubMed PMID: 25460167; PMCID: PMC4251836.
[73] V. Van Puyenbroeck, E. Claeys, D. Schols, T.W. Bell, K. Vermeire, A proteomic survey indicates sortilin as a secondary substrate of the ER translocation inhibitor cyclotriazadisulfonamide (CADA), Mol. Cell. Proteomics 16 (2) (2017) 157–167, https://doi.org/10.1074/mcp.M116.061051.
[74] W. Klein, C. Westendorf, A. Schmidt, M. Conill-Cortes, C. Rutz, M. Blohs, M. Beyermann, J. Protze, G. Krause, E. Krause, R. Schulein, Defining a conformational consensus motif in cotransin-sensitive signal sequences: a proteomic and site-directed mutagenesis study, PloS One. 10 (3) (2015). Epub 2015/03/26. doi: 10.1371/journal.pone.0120886. PubMed PMID: 25806945; PMCID: PMC4373898.
[75] S. Shen, P. Zhang, M.A. Lovchik, Y. Li, L. Tang, Z. Chen, R. Zeng, D. Ma, J. Yuan, Q. Yu, Cyclodepsipeptide toxin promotes the degradation of Hsp90 client proteins through chaperone-mediated autophagy, J. Cell. Biol. 185 (4) (2009) 629–639. Epub 2009/05/13. doi: 10.1083/jcb.200810183. PubMed PMID: 19433452; PMCID: PMC2711573.
[76] S. Kaushik, A.M. Cuervo, The coming of age of chaperone-mediated autophagy, Nat. Rev. Mol. Cell Biol. 19 (6) (2018) 365–381, https://doi.org/10.1038/s41580-018-0001-6.
[77] G. Yao, W. Wang, L. Ao, Z. Cheng, C. Wu, Z. Pan, K.e. Liu, H. Li, W.u. Su, L. Fang, Improved total synthesis and biological evaluation of coibamide A analogues, J. Med. Chem. 61 (19) (2018) 8908–8916, https://doi.org/10.1021/acs.jmedchem.8b01141.s002.
[78] D. Graus-Porta, R.R. Beerli, J.M. Daly, N.E. Hynes, ErbB-2, the preferred heterodimerization partner of all ErbB receptors, is a mediator of lateral signaling, EMBO J. 16 (7) (1997) 1647–1655. Epub 1997/04/01. doi: 10.1093/emboj/16.7.1647. PubMed PMID: 9130710; PMCID: PMC1169769.
[79] J.C. Wilkinson, J.V. Staros, Effect of ErbB2 coexpression on the kinetic interactions of epidermal growth factor with its receptor in intact cells, Biochemistry 41 (1) (2002) 8–14, https://doi.org/10.1021/bi015839l.
[80] T.P.J. Garrett, N.M. McKern, M. Lou, T.C. Elleman, T.E. Adams, G.O. Lovrecz, M. Kofler, R.N. Jorissen, E.C. Nice, A.W. Burgess, C.W. Ward, The crystal structure of a truncated ErbB2 ectodomain reveals an active conformation, poised to interact with other ErbB receptors, Mol. Cell 11 (2) (2003) 495–505, https://doi.org/10.1016/S1097-2765(03)00048-0.
[81] Q.-Y. Chen, Y. Liu, H. Luesch, Systematic chemical mutagenesis identifies a potent novel apratoxin A/E hybrid with improved in vivo antitumor activity, ACS Med. Chem. Lett. 2 (11) (2011) 861–865, https://doi.org/10.1021/ml200176m.